Journal Pre-proof

Robust T cell responses to Pfizer/BioNTech vaccine compared to infection and evidence of attenuated peripheral CD8$^+$ T cell responses due to COVID-19

Fei Gao, Vamsee Mallajoysula, Prabhu S. Arunachalam, Kattria van der Ploeg, Monali Manohar, Katharina Röltgen, Fan Yang, Oliver Wirz, Ramona Hoh, Emily Haraguchi, Ji-Yeun Lee, Richard Willis, Vasanthi Ramachandiran, Jiefu Li, Karan Raj Kathuria, Chunfeng Li, Alexandra S. Lee, Mihir M. Shah, Sayantani B. Sindher, Joseph Gonzalez, John D. Altman, Taia T. Wang, Scott D. Boyd, Bali Pulendran, Prasanna Jagannathan, Kari C. Nadeau, Mark. M. Davis

PII: S1074-7613(23)00125-5

DOI: https://doi.org/10.1016/j.immuni.2023.03.005

Reference: IMMUNI 5051

To appear in: *Immunity*

Received Date: 20 July 2022

Revised Date: 5 January 2023

Accepted Date: 10 March 2023

Please cite this article as: Gao, F., Mallajoysula, V., Arunachalam, P.S., van der Ploeg, K., Manohar, M., Röltgen, K., Yang, F., Wirz, O., Hoh, R., Haraguchi, E., Lee, J.-Y., Willis, R., Ramachandiran, V., Li, J., Kathuria, K.R., Li, C., Lee, A.S., Shah, M.M., Sindher, S.B., Gonzalez, J., Altman, J.D., Wang, T.T., Boyd, S.D., Pulendran, B., Jagannathan, P., Nadeau, K.C., Davis, M.M., Robust T cell responses to Pfizer/BioNTech vaccine compared to infection and evidence of attenuated peripheral CD8$^+$ T cell responses due to COVID-19, *Immunity* (2023), doi: https://doi.org/10.1016/j.immuni.2023.03.005.

Spheromer

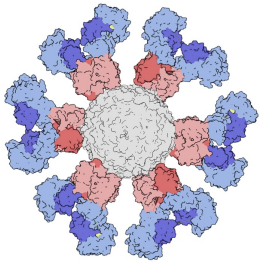

peptide-MHC multimer

oV-2 genome

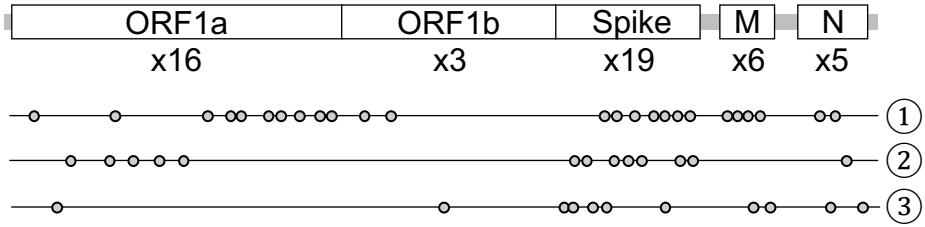

① HLA-A*02:01, ② HLA-B*40:01 and ③ HLA-DRB1*15:01 restricted epitopes

Unexposed subjects receiving Pfizer/BioNTech vaccine

COVID-19 patients

Recovered COVID-19 patients receiving Pfizer/BioNTech vaccine

Magnitude of circulating SARS-CoV-2 specific T cells

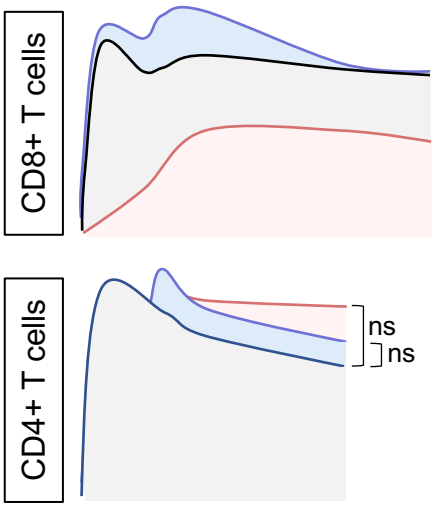

T cell memory distribution

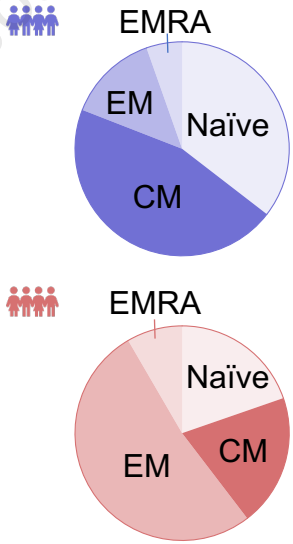

CD8⁺ T cell function

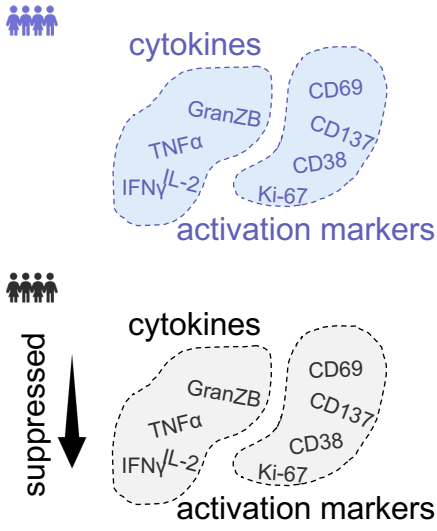

Robust T cell responses to Pfizer/BioNTech vaccine compared to infection and evidence of attenuated peripheral CD8$^+$ T cell responses due to COVID-19

Fei Gao[1‡], Vamsee Mallajoysula[1‡], Prabhu S. Arunachalam[1], Kattria van der Ploeg[7], Monali Manohar[3], Katharina Röltgen[4], Fan Yang[4], Oliver Wirz[4], Ramona Hoh[4], Emily Haraguchi[4], Ji-Yeun Lee[4], Richard Willis[2], Vasanthi Ramachandiran[2], Jiefu Li[1], Karan Raj Kathuria[1], Chunfeng Li[1], Alexandra S. Lee[3], Mihir M. Shah[3], Sayantani B. Sindher[3], Joseph Gonzalez[6], John D. Altman[2,5], Taia T. Wang[6,7], Scott D. Boyd[3,4], Bali Pulendran[1,4,6], Prasanna Jagannathan[6,7], Kari C. Nadeau[1,3,8], and Mark. M. Davis[1,6,9*]

Lead contact: Mark. M. Davis (mmdavis@stanford.edu).

[1] Institute for Immunity, Transplantation, and Infection, Stanford University School of Medicine, Stanford, CA, USA.

[2] Emory Vaccine Center, Emory University School of Medicine, Atlanta, GA, USA.

[3] Sean N. Parker Center for Allergy and Asthma Research, Stanford University and Division of Pulmonary, Allergy, Critical Care Medicine, Stanford University School of Medicine, Stanford, CA, USA.

[4] Department of Pathology, Stanford University School of Medicine, Stanford, CA, USA

[5] Department of Microbiology and Immunology, Emory University School of Medicine, Atlanta, GA, USA

[6] Department of Microbiology and Immunology, Stanford University, Stanford, CA, USA

[7] Department of Medicine, Division of Infectious Diseases, Stanford University, Stanford, CA, USA.

[8]Department of Environmental Health, Harvard T.H. Chan School of Public Health, Harvard, MA, USA

[9] Howard Hughes Medical Institute, Stanford University, Stanford, CA, USA

[*] Correspondence to: mmdavis@stanford.edu

[‡] These authors contributed equally to this work

Summary

T cells are a critical component of the response to SARS-CoV-2, but their kinetics after infection and vaccination are insufficiently understood. Using “spheromer” peptide-MHC multimer reagents, we analyzed healthy subjects receiving two doses of the Pfizer/BioNTech BNT162b2 vaccine. Vaccination resulted in robust Spike-specific T cell responses for the dominant $CD4^+$ (HLA-DRB1*15:01/S191) and $CD8^+$ (HLA-A*02/S691) T cell epitopes. Antigen-specific $CD4^+$ and $CD8^+$ T cell responses were asynchronous, with the peak $CD4^+$ T cell responses occurring one week post the second vaccination (boost), whereas $CD8^+$ T cells peaked two weeks later. These peripheral T cell responses were elevated compared to COVID-19 patients. We also found that prior SARS-CoV-2

infection resulted in decreased $CD8^+$ T cell activation and expansion, suggesting that prior infection can influence the T cell response to vaccination.

Introduction

The COVID-19 pandemic has resulted in the rapid development of several novel vaccine platforms, including the mRNA-based Pfizer/BioNTech BNT162b2 vaccine[1,2]. The mRNA vaccine formulations show high levels of protection and stimulate robust innate and adaptive immune responses[3-6]. They induce neutralizing antibodies, although circulating titers decrease after just months[5,7]. In contrast, analyses of the magnitude and durability of SARS-CoV-2 specific T cell responses are limited, with most studies relying on bulk measurements after *in vitro* peptide stimulation[4,8]. While rapid and useful, these studies underestimate the frequency of epitope-specific T cells[6] and may not be able to identify specific immunodominant epitopes efficiently. Peptide-major histocompatibility complex (pMHC) multimers address these limitations and provide a more quantitative and epitope-specific picture of the T cell response[9-12].

T cell responses play a critical role in controlling disease after SARS-CoV-2 infection. Breakthrough virus in the nasal swabs is seen in all convalescent rhesus macaques with waning or suboptimal neutralizing antibody titers upon rechallenge with SARS-CoV-2 after $CD8^+$ T cell depletion[13]. Recovery from COVID-19 in patients undergoing B cell depleting therapies further highlights the importance of T cells in SARS-CoV-2 viral clearance[14]. $CD8^+$ T cell responses to conserved coronavirus epitopes correlate with mild COVID-19 disease symptoms[15]. Rapid expansion of cross-reactive T cells is also seen in individuals with abortive SARS-CoV-2 infection, suggesting their protective role[16]. Thus, it is important to understand the kinetics of T cell priming, and how these events compare across SARS-CoV-2 naïve vaccinees versus COVID-19 patients.

In this study, we used the spheromer technology to identify dominant T cell epitopes after BNT162b2 vaccination. This platform is based on an engineered form of maxiferritin, where 12 pMHCs carried by each nanoparticle are able to detect ~3-5-fold more antigen-specific T cells compared to other multimers[15]. Here, we designed a panel of forty-nine predicted epitopes, spanning both spike and non-spike proteins from the original Wuhan-Hu-1 SARS-CoV-2 strain. We probed a total of 351 blood samples collected from vaccinated volunteers with timepoints ranging from pre-vaccination up to 4 months after the first dose. Overall, BNT162b2 vaccination resulted in polyfunctional $CD8^+$ and $CD4^+$ T cell responses across all volunteers, likely contributing to its remarkable efficacy. We observed distinct $CD8^+$ and $CD4^+$ T cell kinetics after mRNA vaccination. This disparity between the two major T cell responses is unusual, since in other vaccination studies both $CD4^+$ and $CD8^+$ peak in circulation approximately one week after stimulating a recall response[17-19]. This coordination of T cell subsets was also seen in a Celiac challenge study[20]. We speculate that this may be a unique feature of mRNA vaccines. To assess the differences in T cell responses elicited by vaccination versus natural infection, we determined the response in two independent local patient cohorts[15,21,22]. We observed lower frequencies of spike-specific T cells in circulation after infection compared to mRNA vaccination, especially in the $CD8^+$ T cell compartment with a skewing of the response hierarchy amongst the tested epitopes. We also noticed qualitative differences in the virus-specific T cells. Vaccination led to the rapid induction of effector T cells that contracted by day 90, concomitant with an increase in the frequency of memory T cells. In contrast, only low-levels of virus-specific memory $CD8^+$ T cells could be detected in COVID-19 patients, even at 5 months post symptom onset.

We also evaluated the impact of BNT162b2 vaccination on T cell responses after SARS-CoV-2 infection. While prior infection had almost no effect on the $CD4^+$ T cell response induced upon vaccination, we observed a decrease (3.6 to 54.1-fold at peak) in the frequency of circulating spike-specific $CD8^+$ T cells, and these had attenuated functionality compared to naïve vaccinees. This suggests that SARS-CoV-2 virus infection may cause long-term damage to the patients' immune system well after viral clearance.

Results

The BNT162b2 vaccine encodes a stabilized spike protein from SARS-CoV-2 (Wuhan-Hu-1 strain)[1]. To analyze the T cell responses, we selected nineteen epitopes across multiple HLA alleles spanning the entire spike protein of 1273 amino acids. In addition to five HLA-A*02:01 epitopes used previously for characterizing the response in a COVID-19 patient cohort[15], we included two more HLA-A*02:01 epitopes and seven HLA-B*40:01 epitopes to measure $CD8^+$ T cell responses **(Table S1)**. For the $CD4^+$ T cell response we selected five HLA-DRB1*15:01 epitopes **(Table S1)**. Additionally, we analyzed thirty non-spike epitopes from three different SARS-CoV-2 genes (for $CD8^+$ T cells restricted to HLA-A*02:01 – ORF1ab = 12, M = 4, N = 2; and HLA-B*40:01 – ORF1ab = 5, N = 1; for $CD4^+$ T cells restricted to HLA-DRB1*15:01 – ORF1ab = 2, M = 2, N = 2) in infected individuals **(Table S1)**. Briefly, these peptides were selected based on a combination of the following criteria: literature search[6,9-12,15,24-27], bioinformatic analysis[28-30], and an MHC stabilization assay[15].

Previously, we described spheromers, an improved 12 pMHC T cell staining platform that has superior sensitivity versus other pMHC-multimers[15]. We used our SARS-CoV-2 specific spheromers to characterize the T cell response kinetics in three independent cohorts: (1) SARS-CoV-2 naïve individuals who received the BNT162b2 vaccine, (2) COVID-19 patients with SARS-CoV-2 infections, and (3) Individuals who received the BNT162b2 vaccine after recovery from a SARS-CoV-2 infection. Blood was collected at the indicated timepoints**.** Combinatorial staining was performed as described previously, to probe for multiple specificities[15,31].

We first measured the spike-specific $CD8^+$ T cell response in SARS-CoV-2 naïve vaccinees to estimate the response kinetics to the vaccine. The samples were collected from individuals on day 0 (within 12h of the first dose) and subsequently followed up to 4 months with blood draws **(Fig. 1A)**. PBMCs from unvaccinated individuals collected at least 1 year prior to the pandemic were used to ascertain the baseline frequency to SARS-CoV-2 epitopes. We tested fourteen epitopes across HLA-A*02:01 and HLA-B*40:01 alleles spanning the entire spike sequence **(Fig. 1B-D and Table S1)**. On day 0, SARS-CoV-2 specific $CD8^+$ T cells were detectable with total HLA-A*02:01 anti-spike responses ranging between ~0.007-0.1% **(Figs. 1C)**, similar to that observed in pre-pandemic samples. We observed an extremely rapid mobilization of antigen-specific $CD8^+$ T cells **(Fig. 1E)**. The efficient induction of the immune response after mRNA vaccination resulted in a 36.2-fold increase in spike-specific $CD8^+$ T cells post first dose, consistent with a previous report[11] **(Fig. 1E)**. The frequency of total spike-specific $CD8^+$ T cells increased from 0.31% at baseline to 10.5% before the second dose **(Fig. 1E)**. High frequencies of HLA-A*02:01 spike-specific $CD8^+$ T cells persisted for several weeks after

the second dose with the nominal peak at day 42 **(Fig. 1E)**. At day 42, 19.9% $CD8^+$ T cells were specific for the HLA-A*02:01 epitopes tested. A 5.2-fold contraction was observed by days 42-120, but the frequencies remained high in comparison versus day 0 **(Fig. 1E)**. We also measured the response to seven distinct HLA-B*40:01 spike epitopes **(Fig. 1D)** and observed similar kinetics, with a 44.6-fold increase in the frequency of HLA-B*40:01-restricted spike-specific $CD8^+$ T cells after the first dose **(Fig. 1H)**. The frequencies went up further following the second dose of vaccination **(Fig. 1H)**. However, the magnitude of spike-specific response to the HLA-B*40:01 epitopes was lower than that observed for HLA-A*02:01 **(Fig. 1E, H),** showing that some alleles may be much better at stimulating T cell responses than others. The spike-specific $CD8^+$ T cell response was inversely correlated with age but did not show an association with sex **(Figs.1G, J and S1A-B)**.

The $CD8^+$ T cell response to different epitopes varied considerably **(Figs. 1C-D),** Nevertheless we observed very similar kinetics for all the tested epitopes **(Figs. 1C-D)**. S691 was the most prominent among the seven HLA-A*02:01 epitopes, with a peak median frequency of 7.5% of the $CD8^+$ T cells **(Figs. 1C, F** and **S2A-B)**. The epitope S976, well conserved across hCoVs, also contributes prominently to the overall response with a peak median frequency of 4.6% **(Fig. 1C)**. The rest of the HLA-A*02:01 epitopes had lower frequencies at peak, from 0.5% to 2.2% **(Fig. 1C)**. Among the seven HLA-B*40:01 epitopes, S1016 was the most dominant, peaking at 3.1%, while other epitopes ranged from 0.15% to 0.28% **(Figs. 1D, I** and **S2B)**. The baseline epitope-specific $CD8^+$ T cell response is strongly correlated with the epitope conservation across seasonal human coronaviruses (hCoVs), whereas the peak epitope-specific $CD8^+$ T cell

154 frequencies demonstrated a moderate correlation with epitope conservation across
155 seasonal hCoVs **(Figs. S1D-E).** Our results suggest that mRNA vaccination can induce
156 robust responses to novel spike epitopes and is not limited to cross-reactive specificities
157 imprinted from past seasonal hCoV exposures.

158 Next, we evaluated the functional capacity of the antigen-specific $CD8^+$ T cells
159 following peptide stimulation. PBMC samples collected at day 42 were stimulated with
160 peptides corresponding to the dominant epitopes identified in this study, HLA-
161 A*02:01/S691 and HLA-B*40:01/S1016. After stimulation, we performed cytokine profiling
162 by intracellular staining (ICS) of pMHC-spheromer+ $CD8^+$ T cells **(Figs. 1K, M)**. Most
163 antigen-specific cells made IFNγ and were also able to produce TNFα and IL-2. A minor
164 subset also produced Granzyme B. We also measured activation induced markers (AIM)
165 **(Figs. 1L, N)**. As shown, the dominant epitopes induced the expression of multiple
166 activation markers; CD69, CD154, CD137, CD38 and a marker of proliferation, Ki-67.
167 This durable and stable induction of polyfunctional $CD8^+$ T cells might contribute to the
168 high efficacy of mRNA vaccines.

169 We also surveyed the spike-specific $CD4^+$ T cell response after vaccination **(Figs.**
170 **2A-B** and **Table S1)**. At day 0, the frequency of epitope-specific $CD4^+$ T cells ranged from
171 0.05-0.07%, that was comparable to the levels in pre-pandemic samples **(Fig. 2C)**. We
172 observed a rapid increase in the frequencies of spike-specific $CD4^+$ T cells within a week
173 after the first dose **(Fig. 2D)**. The second dose led to a smaller increase (2.3-fold) in the
174 overall anti-spike $CD4^+$ T cell response **(Fig. 2D)**. However, in contrast to the $CD8^+$ T
175 cells, a decrease in the circulating anti-spike $CD4^+$ T cells was observed by day 42 **(Fig.**

2D). This discordance in the kinetics of the major T cell subsets may relate to the distinct functions they execute. Even so, spike-specific $CD4^+$ T cells were detectable at higher frequencies in circulation in comparison to day 0, even three months after vaccination **(Fig. 2D)**. Among the tested epitopes, the most dominant response was observed against S191, with a median frequency of 9.7% on day 28 **(Figs. 2C, E** and **S2B)**. The other epitopes varied between 1.5% to 2.9% **(Fig. 2C)**. The kinetics of $CD4^+$ T cells specific to the dominant epitope, S191, followed the total spike response **(Fig. 2E)**. As with the $CD8^+$ T cells, the $CD4^+$ T cell response was decreased in older individuals but showed no sex association (**Figs. 2F** and **S1C**). The total spike-specific and dominant S191 epitope-specific $CD4^+$ T cell response kinetics further correlated with SARS-CoV-2 spike-specific IgG levels **(Fig. 2G)**.

We next evaluated the cytokine profile of spike-specific $CD4^+$ T cells after stimulating day 28 PBMCs with the dominant peptide, S191. The pMHC-spheromer+ $CD4^+$ T cells produced IFNγ, TNFα, IL-2 and Granzyme B, indicating a Th1-skewing as reported previously[32] **(Fig. 2H)**. These cells also expressed multiple activation markers after stimulation, further validating the functional capacity of vaccine induced $CD4^+$ T cells **(Fig. 2I)**. In contrast to the $CD8^+$ T cell response, the epitope conservation across seasonal hCoVs did not correlate with the baseline or peak CD4+ T cell frequencies, which suggests that the vaccine induced responses to novel SARS-CoV-2 epitopes (**Figs. S1F-G**). Taken together, these robust T cell responses induced by the BNT162N2 mRNA vaccine likely contributes to its remarkable efficacy.

To study the development of anti-SARS-CoV-2 $CD8^+$ T cell immunity mediated by vaccination versus natural infection, we compared the responses of SARS-CoV-2 naïve vaccinees and COVID-19 patients. The patient samples were grouped by days since symptom onset and matched with samples from BNT162b2 vaccinees as indicated **(Fig. 3A)**. The patient cohort was established during the first wave of the pandemic (June~December 2020) and were most likely infected by the Wuhan-Hu-1 SARS-CoV-2 strain that matches the vaccine formulation. To perform an integrated analysis, we compiled 12 features of spike-specific $CD8^+$ T cell response derived from flow assays **(Fig. S3A)**. Overall, BNT162b2 vaccination and SARS-CoV-2 infection resulted in distinct spike-specific $CD8^+$ T cells profiles indicated by non-overlapping clusters in UMAP space. We observed divergent spike-specific $CD8^+$ T cell response after vaccination and infection in terms of the preferred epitopes **(Fig. S3B)**. While the dominant epitope within spike protein in vaccinees is S691, the main response after infection were against S976 and S983, with a median peak frequency of 0.25% and 0.24%, respectively **(Fig. S3B)**. The total spike-specific $CD8^+$ T cell response in circulation elicited by infection was lower in magnitude in comparison to vaccination **(Fig. S3C)**. After a single vaccine dose (T1), the spike-specific $CD8^+$ T cell response in circulation was 40.6-fold higher than natural infection **(Fig. S3C)**. This difference in median frequency after the second dose of vaccination (T2) ranged from 9.5 to 21.6-fold **(Fig. S3C)**. The response to S691 in the COVID-19 patient cohort, the dominant epitope in vaccinated individuals, was 25.1 to 143.4-fold lower across the sampled timepoints **(Fig. S3D)**. As for durability, anti-spike $CD8^+$ T cells were detectable at higher frequencies in circulation in comparison to COVID-19 patients even during the contraction phase (T3 and T4) of the immune response **(Figs.**

S3C-D). BNT162b2 vaccination induces a T cell response exclusively to spike peptides since the vaccine encodes only that protein. In contrast, SARS-CoV-2 infection generates a response against the whole virus[8]. Therefore to capture that response, we tested eighteen additional epitopes derived from three different genes **(**ORF1ab = 12, M = 4, and N = 2) **(Fig. 3B)**. The magnitude of T cell response to both spike and non-spike epitopes in COVID-19 patients was comparable **(Fig. 3C, D)**. At the nominal peak after vaccination (T2), the $CD8^+$ T cell response (spike-only) in naïve vaccinees was 10.6-fold higher than that in COVID-19 patients (spike and non-spike epitopes) **(Fig. 3E)**. We also performed peptide mega pool (MP) stimulation assay since it enables profiling a much broader landscape of T cell responses. We did not observe any difference in the response to spike and non-spike peptide pools among COVID-19 patients **(Figs. 3F** and **S4A)**. In contrast to pMHC-spheromer staining **(Figs. 3F** and **S4A)**, we observed a slight but not significant 1.3-fold decrease in the $CD8^+$ T cell response to spike peptide pool stimulation in COVID-19 patients in comparison to vaccinees by AIM assay **(Figs. 3F** and **S4A)**. This discrepancy between pMHC-spheromer staining and AIM assay could in part be due to limitation of the peptide stimulation assay to capture all relevant T cells due to the relative lack of sensitivity. We recently observed that *Mycobacterium tuberculosis* (*Mtb*) MP captures only a fraction (33.6%) of the total T cell response defined by TCR specificity groups identified from the analysis of 19,044 unique TCRβ sequences derived from individuals with latent Mtb infection using GLIPH2 algorithm[33]. To investigate this further, we performed stimulation with the dominant $CD8^+$ spike peptide (A2/S691) and evaluated the T cell response using both pMHC-spheromer and AIM markers in 16 vaccine donors **(FigS. S4C-D)**. This allowed us to directly compare pMHC-spheromer$^+$ and AIM^+ $CD8^+$ T

cell responses. We found that pMHC-spheromers captured most (94.6 ± 9.5%) AIM^+ $CD8^+$ T cells **((Fig. S4C)**. In contrast, only a fraction (18.1 ± 10.1%) of all pMHC-$spheromer^+$ cells were positive for both CD69 and CD137 **(Fig. S4C)**. For the dominant spike peptide, pMHC-spheromers detect 9.5-fold more epitope-specific $CD8^+$ T cells compared to the AIM assay **((Fig. S4D)**. Thus, we speculate that stimulation assays are able to capture only a fraction of the total responses compared to pMHC-spheromers.

Next, we characterized the memory T cell compartment in these cohorts. The absolute number of total memory $CD8^+$ T cells at early timepoints (T1 and T2) was similar between the two cohorts **(Fig. 3G)**. The total memory $CD8^+$ T cell counts during late convalescence in COVID-19 patients was 1.3-fold and 1.4-fold lower compared to vaccinated individuals at T3 and T4, respectively **(Fig. 3G)**. We next measured the spike-specific T cell memory subset distribution **(Fig. 3H)**. Antigen mediated activation of spike-specific $CD8^+$ T cells after vaccination led to an effector phenotype ($CD45RA^{+/-}CCR7^-$). The progressive contraction of effector cells after vaccination was coupled with the establishment of robust central memory ($CD45RA^+CCR7^-$) **(Fig. 3H)**. In contrast, infection resulted in chronic activation of spike-specific $CD8^+$ T cells, with effector cells ($CD45RA^-$ $CCR7^-$) dominating the early to late convalescent phase **(Fig. 3H)**.

We also measured the effect of BNT162b2 vaccination or SARS-CoV-2 infection on $CD4^+$ T cells **(Fig. 4A)**. The distinct route of exposure to viral antigens, that is vaccination or infection, resulted in non-overlapping spike-specific $CD4^+$ T cell clusters, again suggesting a divergent T cell response **(Fig. S3E)**. However, we did not observe any shift in the favored spike epitope between vaccinees and COVID-19 patients, with both the cohorts focused on S191 **(Fig. S3F)**. The magnitude of spike-specific peripheral

CD4$^+$ T cells induced by vaccination demonstrated higher flux than in COVID-19 patients **(Fig. S3G)**. A single dose of the vaccine (T1) resulted in similar frequencies of spike-specific CD4$^+$ T cells as SARS-CoV-2 infection **(Fig. S3G)**, but the second dose of the vaccine resulted in 3.3-fold higher response in naïve vaccinees versus COVID-19 patients **(Fig. S3G)**. At later time points (T3 and T4), the spike-specific CD4$^+$ T cells in vaccinees dropped to be comparable to COVID-19 patients **(Fig. S3G)**. The response to the dominant epitope (S191) followed the same kinetics as the total CD4$^+$ T cell response **(Fig. S3H)**. We also measured the CD4$^+$ T cell response to non-spike epitopes (ORF1ab = 2, M = 2, and N = 2) in COVID-19 patients **(Figs. 4B-C)** and found that they were comparable to the spike epitopes **(Fig. 4D)**. The CD4$^+$ T cell response between COVID-19 patients (spike and non-spike) and naïve vaccinees (spike only) was comparable at all timepoints except at T4 **(Fig. 4E)**. We did not observe any difference in the CD4$^+$ T cell activation between COVID-19 patients and naïve vaccinees by AIM assay at the nominal peak (T2) post vaccination **(Fig. 4F)**.

However, we saw a marked difference in memory CD4$^+$ T cells between the two cohorts. While we saw higher frequencies of antigen-specific CD4$^+$ T cells in COVID-19 patients during late convalescence (T4), there was a reduction in the total memory CD4$^+$ T cells at these timepoints (T3 and T4) compared to naïve vaccinees **(Fig. 4G)**. Analogous to the CD8$^+$ T cell response, mRNA vaccination resulted in the rapid recruitment of spike-specific effector CD4$^+$ T cells (CD45RA$^{+/-}$CCR7$^-$) **(Fig. 4H)**. The contraction of effector cells was concomitant with central memory (CD45RA$^+$CCR7$^-$) spike-specific CD4$^+$ T cells **(Fig. 4H)**. In contrast, natural infection resulted in a more even distribution of spike-specific CD4$^+$ T cells across the effector (CD45RA$^-$CCR7$^-$) and central memory

289 (CD45RA$^+$CCR7$^-$) subsets throughout convalescence **(Fig. 4H)**. Taken together, these
290 results suggest differences in how CD8$^+$ and CD4$^+$ T cell response are triggered by
291 SARS-CoV-2 infection versus BNT162b2 vaccination. While we cannot exclude the
292 possibility of virus-specific T cell localization in the lung during the course of an infection
293 for the noticeably lower circulating spike-specific CD8$^+$ T cells[34], this difference could also
294 be a consequence of the virus's ability to dampen protective host immune responses via
295 the inhibition of MHC-I expression[35-37].

296 We also investigated the effect on mRNA vaccination in subjects who had
297 previously recovered from SARS-CoV-2 infection **(Figs. 5A-B)**. Not surprisingly, the
298 major response in these individuals was to the spike epitopes **(Figs. 5C-D)** which were
299 12.5-fold (at day 42) and 11.3-fold (at day 28) higher than non-spike epitopes for CD8$^+$
300 and CD4$^+$ T cells, respectively **(Figs. 5E, I)**.

301 As with SARS-CoV-2 naïve individuals, the dominant CD8$^+$ T cell response was
302 against HLA-A*02:01/S691 and HLA-B*40:01/S1016 **(Fig. 5C)**. However, the total
303 peripheral CD8$^+$ T cell response in convalescent individuals after vaccination was 5.5-fold
304 lower than naïve vaccinees after the first dose (day 21) **(Fig. 5F)**. Furthermore, we
305 observed minimal boosting of the CD8$^+$ T cell response after the second dose of
306 vaccination, resulting in 7.3-fold lower CD8$^+$ T cell levels in circulation in comparison to
307 naïve vaccinees at day 42 **(Fig. 5F)**. In contrast, there was no dampening of specific CD4$^+$
308 T cell responses between the SARS-CoV-2 naïve and pre-exposed individuals (**Fig. 5J)**.
309 We also performed a detailed characterization of the spike-specific CD8$^+$ and CD4$^+$ T cell
310 response kinetics in a subset of these individuals **(Fig. S5A)**. We noticed that prior

infection did not affect the early spike-specific $CD8^+$ T cell response (day 0-7) **(Fig. S5B)**. However, attenuation of the circulating $CD8^+$ response was apparent by day 21. The boost in the $CD8^+$ T cell response after the second dose was minimal and could be due to faster response kinetics in convalescent individuals in comparison to naïve vaccinees as previously reported[38]. This could also contribute to the difference in the total $CD8^+$ T cell response (spike and non-spike) which was maximum at day 42 **(Fig. 5F)**. This difference in the spike-specific $CD8^+$ T cell response was no longer significant three months after the first vaccination (**Fig. S5B**). This suggests that BNT162b2 vaccination can partially rescue the lower circulating $CD8^+$ T cell responses observed after SARS-CoV-2 infection. The decrease in the magnitude of circulating spike-specific $CD8^+$ T cells after vaccination in recovered COVID-19 patients was also associated with reduced functionality. PBMCs (day 42) stimulated with spike peptides (S691 or S1016) had a reduced capacity to produce cytokines such as IFNγ, TNFα and IL-2 and dampened cytotoxic potential (Granzyme B) **(Fig. 5G)**. They were also refractory to activation as seen by the lower expression of multiple activation markers such as CD69, CD137, CD38 and Ki-67, but not CD154 **(Fig. 5H)**. However, we did not observe any impaired functionality of spike-specific $CD4^+$ T cell responses after vaccination **(Figs. S5C** and **5K-L)**. Overall, our results show that SARS-CoV-2 infection impairs $CD8^+$ T cell responses to the BTN162b2 vaccine but not $CD4^+$ T cell responses.

Lastly, the emergence of several new SARS-CoV-2 variants raises the question of immune evasion. A high degree of functional preservation is seen in memory T cell responses against early SARS-CoV-2 variants by the AIM assay[39]. 84% ($CD4^+$) and 85% ($CD8^+$) of the memory T cell response induced upon vaccination with the Wu-1 strain is

preserved against the Omicron variant (B.1.1.529)[39]. However, multiple lineages of the Omicron (B.1.1.529) variant have since emerged that escape from vaccine or infection induced neutralizing antibodies[40]. Therefore, we analyzed the conservation of predicted spike-derived T cell epitopes from the Wu-1 strain across the SARS-CoV-2 variants, including the subvariants BA.4 and BA.5 **(Figs. 6A-C)**. Overall, the T cell epitopes are fairly conserved across all the analyzed variants, with an average total conservation score of 90.3% and 90.8% for HLA-A*02:01 and HLA-B*40:01, respectively **(Figs. 6A-B)**. The average total conservation score for HLA-DRB1*15:01 restricted T cell epitopes was marginally lower (84.6%) **(Fig. 6C)**. The omicron subvariant BA.4 and BA.5 had the least conservation of both $CD8^+$ and $CD4^+$ T cell epitopes compared to the Wu-1 strain **(Figs. 6A-C)**. A total conservation of 88% for both HLA-A*02:01 and HLA-B*40:01 T cell epitopes was observed between Wu-1 and omicron subvariant BA.4 and BA.5 **(Figs. 6A-B)**, as opposed to only 74% for HLA-DRB1*15:01 **(Fig. 6C)**. These results indicate that continued virus evolution could attenuate T cell responses. But the epitopes we tested in this study are fairly conserved across all variants **(Figs. 6D-F).** The dominant epitopes, HLA-A*02:01/S691 and HLA-DRB1*15:01/S191 are completely conserved across all analyzed variants including BA.4 and BA.5 **(Figs. 6D-E)**. HLA-B*40:01/S1016 is 97.6% conserved across all variants **(Fig. 6F)**. Presently, the BQ and XBB subvariants of SARS-CoV-2 Omicron are spreading rapidly across the globe and their neutralization by sera from vaccinees and infected individuals is low[41]. Even so, the dominant epitopes for HLA-A*02:01/S691, HLA-B*40:01/S1016 and HLA-DRB1*15:01/S191 as described here are completely conserved in these variants. In this context, Poon et. al. monitored the viral

diversity in individuals after vaccination and observed that T cell responses do not appear to have a substantial impact on the emergence of these recent viral variants[42].

Discussion

The SARS-CoV-2 pandemic has had an enormous health and economic impact worldwide and thus a detailed investigation of the mechanisms mediating the high efficacy of the novel RNA vaccines[3-5,8-12] is warrented and should help in the design of vaccines against other pathogens. Using spheromer technology[15], we probed the kinetics and durability of epitope-specific $CD8^+$ and $CD4^+$ T cell responses after mRNA vaccination in naïve and COVID-19 patients. Spheromers can detect ~3-5-fold more specific T cells than tetramers[15]. Here, we analyzed the response to the BNT162b2 vaccine and observed a rapid induction of $CD8^+$ and $CD4^+$ T cells, with an increase in the total HLA-A*02:01 spike-specific response as early as day 1 after vaccination. Here, extending previous results with CD8 T cells[11], we surveyed multiple epitopes and also $CD4^+$ T cell specificities. Previously we found that the frequency of SARS-CoV-2 specific $CD8^+$ T cells in unexposed individuals correlates with epitope conservation across seasonal hCoVs[15]. We saw a similar correlation in spike-specific $CD8^+$ T cells and sequence conservation prior to vaccination here, but by day 42 post vaccination, there was only a weak correlation with epitope conservation. Specifically, the dominant $CD8^+$ T cell response at the nominal peak (day 42) was against HLA-A*02:01/S691 and HLA-B*40:01/S1016 with frequencies of 7.5% and 3.1%, respectively. These results suggest that mRNA vaccination can efficiently induce a response to novel spike epitopes. Antonio et. al. found a high degree of structural convergence of physico-chemical properties of A2/S691

peptide with the immunodominant influenza virus matrix epitope (A2/M1) despite poor sequence conservation[43]. TCRs that are specific to both influenza-M1 and SARS-CoV-2 antigens have also been reported[44]. This cross-reactivity may explain the higher response we observed against A2/S691 in comparison to A2/S269. With respect to the $CD4^+$ T cell response, the dominant HLA-DRB1*15/S191 epitope constituted 9.7% of all $CD4^+$ T cells at the nominal peak (day 28). This observation of a higher spike-specific $CD4^+$ T cell response compared to $CD8^+$ T cells is consistent with previous studies[3,4]. However, in contrast to results from peptide pool stimulation[3], with pMHC-spheromers we found that the $CD4^+$ and $CD8^+$ responses did not follow the same kinetics. The $CD4^+$ T cell kinetics were synchronous with the spike-specific antibody response, with the peak at day 28 (one week after the second dose) followed by a contraction. In contrast, we observed a steady increase in the antigen-specific $CD8^+$ T cell response all the way up to day 42 (3 weeks post the second dose). This discordance is unusual compared to other studies where both $CD4^+$ and $CD8^+$ responses peak in the blood about 6-8 days post stimulation in a memory response[17-20]. This may be due to the distinct features of the mRNA vaccine platform. This prolonged induction of $CD8^+$ T cells after vaccination may also relate to the striking increase in IFNγ levels observed after the second dose of BNT162b2 vaccine[3,45] as opposed to an earlier cytokine surge observed with other vaccines. Although the frequency of spike-specific $CD8^+$ and $CD4^+$ T cells in circulation decreased with time in comparison to the peak levels, they were still detectable 3-4 months after vaccination, indicating a durable T cell response. An elegant study by Mudd et. al.[10] shows the persistence of spike-specific T follicular helper cells (DP4/S167) in the lymph nodes at a relatively higher frequency in comparison to peripheral circulation at matched timepoints.

The considerable longitudinal sampling of vaccinees further allowed us to study the development of T cell memory. Although, we observed differences in the magnitude of response to distinct spike epitopes, the formation of $CD8^+$ and $CD4^+$ T cell memory after vaccination was quite similar across different epitopes. Overall, there was an increase in antigen-specific effector T cells (CCR7-$CD45RA^{+/-}$) by day 21 that contracted to nearly pre-vaccination levels by day 90. Concomitantly, the spike-specific T cells in circulation after 3-4 months post vaccination exhibited a central memory phenotype ($CCR7^+CD45RA^-$). This is important since a stable memory pool could effectively protect against future SARS-CoV-2 infections by their rapid recruitment in the immune response.

We also compared T cell responses after vaccination to natural infection. We found that the circulating antigen-specific $CD8^+$ T cell response was much lower in SARS-CoV-2 infection versus vaccination. Specifically, the nominal peak post vaccination was 10.6-fold higher than in infected individuals, and decreased to 4.3-fold at 4 months after vaccination for spike-specific responses. We also observed a skewing in the preferred $CD8^+$ T cell epitopes targeted after infection in comparison to vaccination, with the maximal spike response against HLA-A*02:01/S976 with a median frequency of 0.25% at peak. The difference in preferred spike specificities between the two cohorts is likely due to differences in antigen localization, processing and presentation after infection versus vaccination. The infection induced spike-specific $CD4^+$ T cell response in circulation were marginally reduced (3.3-fold) at peak in comparison to vaccination, but no difference was observed in the total (spike and non-spike) $CD4^+$ T cell frequencies. This marginal reduction in the spike-specific peripheral $CD4^+$ T cells could explain the lower antibody titers observed in individuals experiencing mild symptoms after SARS-CoV-2 infection in

comparison to the post-vaccination antibody titers observed in SARS-CoV-2 naive vaccinees[46]. The migration of virus-specific T cells after infection to the respiratory tract[34] or lymphopenia after SARS-CoV-2 infection[47] can also cause lower spike-specific T cells in the periphery. We suggest that this may also be a consequence of the virus's strategy to escape host defense by specifically inhibiting the MHC-I expression, as reported recently[35-37]. Here we were only able to analyze peripheral T cells responses, as is a typical limitation of human studies. A recent study using pMHC-multimers did not observe any difference in the frequency of SARS-CoV-2 specific $CD8^+$ T cells between infected and vaccinated individuals[9]. We speculate that this could be a combined effect of the different specificities and timepoints used, both crucial factors as shown here. We also observed that spike-specific $CD8^+$ T cells induced after infection exhibited an effector phenotype even 5 months after symptom onset. This could be a consequence of viral persistence[48]. We suggest that chronic activation probably leads to reduced virus-specifc memory $CD8^+$ T cells in comparison to BNT162b2 vaccination. This may contribute to the increased prevalence of breakthrough SARS-CoV-2 infection in COVID-19 patients as compared to vaccinees seen in some studies. Eggink et. al., observed an increased risk of Omicron infection in previously infected individuals (odds ratio (OR): 4.2; 95% confidence interval (CI): 3.8–4.7) compared with naïve vaccinated individuals. The OR of Omicron infection among vaccinated individuals was 3.6 (95% CI: 3.4–3.7). This is in contrast to susceptibility to infection by other SARS-CoV-2 variants[49]. In another study evaluating protection conferred by mRNA vaccines and previous infection against Omicron in a prison cohort (a high-risk population), the authors observed higher levels of effectiveness from vaccination among staff in comparison to previous infection. However,

447 no difference was observed in the inmates[50]. But it is important to note that these results
448 are contrary to that observed by Altarawneh et. al.[51]. They observed a higher
449 effectiveness of previous infection (alone) against symptomatic BA.2 infection in
450 comparison to two doses of BNT162b2 mRNA vaccine (>6 months before infection) in
451 naïve individuals.

452 We also analyzed the impact of prior SARS-CoV-2 infection on BNT162b2 vaccine
453 induced T cell responses. Previous studies found no deficit in neutralizing antibody titers
454 to the ancestral Wuhan-Hu-1 SARS-CoV-2 strain after vaccination in pre-exposed
455 individuals[5]. Accordingly, we observed no effect on the $CD4^+$ T cell response. But we did
456 observe a major reduction in both the magnitude and functionality of peak $CD8^+$ T cell
457 responses in previously infected individuals after vaccination. This could be a result of the
458 disproportionate effect of infection on the $CD8^+$ T cell compartment in comparison to $CD4^+$
459 T cells, as discussed previously. The deterioration of $CD8^+$ T cell function is seen in
460 patients with active viral infections that had been either eliminated, in the case of HCV or
461 greatly reduced (HIV)[23]. This dysfunction persists for a year or more after the active phase
462 of infection, suggesting lasting damage, despite the absence or near absence of the
463 relevant virus. In this context, it may be that these attenuated $CD8^+$ T cell responses
464 contribute to long COVID, perhaps rendering patients unable to respond robustly to
465 subsequent infections by SARS-CoV-2 variants or other pathogens. Another factor that
466 could contribute to the lower circulating spike-specific T cells in convalescent individuals
467 could be due to the reduced immunogenicity of mRNA vaccine resulting from antigen
468 sequestration mediated by infection induced antibodies in circulation. Previous
469 studies[52,53] have reported higher levels of T cell responsiveness after spike peptide pool

stimulation in vaccinated individuals undergoing treatment with anti-CD20 antibody monotherapy or anti-CD19 CAR T that result in lower spike-specific antibodies in comparison to healthy individuals.

Lastly, we evaluated the conservation of spike-derived T cell epitopes evaluated in this study across SARS-CoV-2 variants. The dominant epitopes identified here are almost completely conserved, including in the BA.4 and BA.5 subvariants. This can be critical since a reduction in the neutralizing antibody titer in comparison to the reference Wu-1 isolate is seen with the omicron subvariants even after the administration of a booster dose (3rd vaccine dose)[40]. The neutralizing antibody titer is lower by a factor of 6.4, 7.0 and 14.1 against BA.1, BA.2, and BA.2.12.1 subvariants, respectively. Furthermore, a 21-fold reduction in the neutralizing antibody titer is seen against the BA.4 and BA.5. Considering this continued viral evolution, the identification of conserved, dominant T cell epitopes as reported here may facilitate the much-needed development of pan-coronavirus vaccines.

In summary, our study elucidates the magnitude, diversity and kinetics of specific $CD4^+$ and $CD8^+$ T cell responses after BNT162b2 vaccination, and the effects of SARS-CoV-2 infection on these responses. It will be interesting to see whether some of the characteristics we see here are a common feature of RNA vaccines to other pathogens. In addition, the apparent damage of the $CD8^+$ T cell response by viral infection is cause for concern, and may leave even vaccinated individuals with a prior infection at risk for subsequent infections or other health issues.

Limitations of the Study

Our study has limitations in that we measured only peripheral T cell responses, and differential tissue localization of immune cells after mRNA vaccination and SARS-CoV-2 infection can contribute to the differences observed between the cohorts. We speculate that virus induced MHC-I suppression drives the specific attenuation of $CD8^+$ T cell responses after infection, but other factors such differential kinetics and spike antigenicity in pre-exposed individuals can also affect $CD8^+$ T cell responses in convalescent individuals. Future studies are warranted to delinate the relative impact of these factors. Finally, although we used a large panel of forty-nine epitopes to characterize the SARS-CoV-2 specific T cell responses, this is not exhaustive and other epitopes might conceivably yield different results.

Figure legends

Figure 1: Vaccine elicited spike-specific $CD8^+$ T cell responses. (A) The experimental design to evaluate the $CD8^+$ T cell response to BNT162b2 vaccination. Timeline showing sequential blood draws post vaccination (first dose (day 0) and second dose (day 21)) in HLA-A*02:01 and HLA-B*40:01 donors. The number of donors (n), age and sex are indicated. **(B)** Fourteen $CD8^+$ T cell epitopes from SARS-CoV-2 spike protein were evaluated. The magnitude of $CD8^+$ T cell responses to distinct SARS-CoV-2 spike epitopes in **(C)** HLA-A*02:01 and **(D)** HLA-B*40:01 vaccinees. Baseline for each epitope is shown by a dotted line, determined using pre-pandemic samples (n=5). Each donor is represented by a dot. Fold-change in the $CD8^+$ T cell response to **(E)** the spike protein and to **(F)** the dominant epitope (S691) in HLA-A*02:01 restricted vaccinees. **(G)**

Correlation between spike-specific $CD8^+$ T cell response at day 42 and age in HLA-A*02:01 donors. The $CD8^+$ T cell response dynamics to **(H)** the spike protein and to **(I)** the dominant epitope (S1016) in HLA-B*40:01 restricted vaccinees. **(J)** Correlation between spike-specific $CD8^+$ T cell response (day 42) and age in HLA-B*40:01 donors. **(K** and **M)** Fraction of cytokine producing $CD8^+$ T cells within **(K)** S691/A*02:01 and **(M)** S1016/B*40:01 specific $CD8^+$ T cells at peak after peptide stimulation. **(L** and **N)** Fraction of cells expressing activation induced markers (AIM) within **(L)** S691/A*02:01 and **(N)** S1016/B*40:01 specific $CD8^+$ T cells at peak after peptide stimulation. Data are presented as mean ± range. The pearson correlation coefficient and statistical significance are noted in **(G)** and **(J)**. See also Figure S1 and S2.

Figure 2. Vaccine elicited spike-specific $CD4^+$ T cell response. (A) The experimental design to evaluate the epitope-specific $CD4^+$ T cell response to BNT162b2 vaccine in longitudinal samples. The number of donors (n), age and sex are indicated. **(B)** Five $CD4^+$ T cell epitopes from SARS-CoV-2 spike protein were evaluated. The magnitude of $CD4^+$ T cell responses to SARS-CoV-2 epitopes in **(C)** HLA-DRB*15:01 vaccinees. Baseline for each epitope is shown (dotted line), determined using pre-pandemic samples (n=5). Each donor is represented by a dot. Fold-change in the $CD4^+$ T cell response to **(D)** the spike protein and to **(E)** the dominant epitope (S191). **(F)** Correlation between spike-specific $CD4^+$ T cell response (day 28) and age. The pearson correlation coefficient and statistical significance are given. **(G)** Pearson correlation between the kinetics of vaccine elicited spike-specific IgG response, total spike-specific $CD4^+$ T cell response (left) and DRB*15:01/S191 specific $CD4^+$ T cell response (right). **(H)** Fraction of cytokine producing

cells within S191/DRB*15:01 specific $CD4^+$ T cells (day 28) after peptide stimulation. **(I)** Fraction of AIM+ $CD4^+$ T cells within S191/DRB*15:01 specific $CD4^+$ T cells (day 28) after peptide (S191) stimulation. Data are presented as mean ± range. See also Figure S1 and S2.

Figure 3. BNT162b2 vaccination and SARS-CoV-2 infection induce distinct $CD8^+$ T cell response. (A) The experimental design to compare the epitope-specific $CD8^+$ T cell response to BNT162b2 vaccine and SARS-CoV-2 infection. Samples were matched by time points for comparison as shown. The number of subjects (n) is indicated. **(B)** The twenty-five evaluated $CD8^+$ T cell epitopes mapped onto the SARS-CoV-2 genome. **(C)** The magnitude of $CD8^+$ T cell responses to SARS-CoV-2 epitopes in HLA-A*02:01 restricted COVID-19 patients. **(D)** The comparison of spike and non-spike specific $CD8^+$ T cell response in COVID-19 patients. **(E)** The comparison of antigen-specific $CD8^+$ T cell response to BNT162b2 vaccine and SARS-CoV-2 infection. Data in panels (C-E) represented as mean ± range. **(F)** Fraction of AIM^+ $CD8^+$ T cells in day 42 samples after spike peptide mega pool (spike MP), non-spike peptide mega pool (non-spike MP) or DMSO stimulation. Data presented as mean ± SD. **(G)** Total memory $CD8^+$ T cell counts in vaccinees and patients. Data presented as mean ± range. **(H)** Antigen-specific memory $CD8^+$ T cell distribution in vaccinees and patients. (CM: central memory; EM: effector memory; EMRA: effector memory T cells expressing CD45RA). Data presented as mean ± range. P-values were determined by Mann–Whitney test with Holm–Šídák method. See also Figure S3 and S4.

Figure 4. BNT162b2 vaccination and SARS-CoV-2 infection elicited CD4⁺ T cell response. (A) The experimental design to compare the epitope-specific CD4⁺ T cell response to BNT162b2 vaccine and SARS-CoV-2 infection. Samples matched for comparison as shown. The number of subjects (n) is indicated. **(B)** The eleven evaluated CD4⁺ T cell epitopes are mapped onto the SARS-CoV-2 genome. **(C)** The magnitude of CD4⁺ T cell responses to SARS-CoV-2 epitopes in COVID-19 patients. **(D)** The comparison of spike and non-spike specific CD4⁺ T cell response in COVID-19 patients. **(E)** The comparison of antigen-specific CD4⁺ T cell response to BNT162b2 vaccine and SARS-CoV-2 infection. Data in panels (C-E) are represented as mean ± range. **(F)** Fraction of AIM+ CD4⁺ T cells in day 28 samples after spike MP, non-spike MP or DMSO stimulation. Data represented as mean ± SD. **(G)** Total memory CD4⁺ T cell counts in vaccinees and patients. Data represented as mean ± range. **(H)** Antigen-specific memory CD4⁺ T cell distribution in vaccinees and patients. Data represented as mean ± range. P-values determined by Mann–Whitney test with Holm–Šídák method. See also Figure S3 and S4.

Figure 5. Reduced peripheral vaccine induced CD8⁺ T cell response in recovered COVID-19 patients. (A) The experimental design to study the CD8⁺ and CD4⁺ T cell responses to BNT162b2 vaccine in individuals recovered from previous COVID-19 infection. Timeline indicating the collection of sequential blood samples from HLA-A*02:01, HLA-B*40:01 (day 21 and day 42) and HLA-DRB1*15:01 (day 21 and day 28) recovered vaccinees. The number of donors (n) is indicated. **(B)** Thirty-eight CD8⁺ T and eleven CD4⁺ T cell epitopes evaluated in this study are mapped onto the SARS-CoV-2

genome. The number of donors (n) is indicated. **(C)** The magnitude of $CD8^+$ T cell responses to SARS-CoV-2 epitopes in HLA-A*02:01 (red) and HLA-B*40:01 (yellow) donors. **(D)** The magnitude of $CD4^+$ T cell responses to SARS-CoV-2 epitopes in HLA-DRB1*15:01 donors. Data in panels (C-D) are represented as mean ± range. **(E)** The comparison of spike and non-spike specific HLA-A*02:01 (red) and HLA-B*40:01 (yellow) $CD8^+$ T cell responses. **(F)** The comparison of HLA-A*02:01 (red) and HLA-B*40:01 (yellow) $CD8^+$ T cell responses to BNT162b2 vaccine in naïve and recovered vaccinees. Data represented as mean ± range. **(G** and **H)** Fraction of **(G)** cytokine producing and **(H)** AIM expressing T cells within S691/A*02:01 and S1016/B*40:01 specific $CD8^+$ T cells (day 42 samples) after peptide stimulation (S691 and S1016, respectively). **(I)** The comparison of spike and non-spike specific $CD4^+$ T cell response in recovered vaccinees. **(J)** The comparison of antigen-specific $CD4^+$ T cell response to BNT162b2 vaccine in naïve and recovered vaccinees. **(K** and **L)** Fraction of **(K)** cytokine producing and **(L)** AIM expressing T cells within S191/DRB*15:01 specific CD4+ T cells (day 28) after peptide stimulation (S191). P-values were determined by Mann–Whitney test with Holm–Šídák method. See also Figure S5.

Figure 6: T cell epitope conservation across SARS-CoV-2 variants. The fractional conservation of all predicted spike-derived T cell epitopes from the SARS-CoV-2 reference Wuhan-1 (Wu-1) strain against the indicated SARS-CoV-2 variant for **(A)** HLA-A*02:01 **(B)** HLA-B*40:01 and **(C)** HLA-DRB1*15:01 are shown. The Pango lineage for each SARS-CoV-2 variant is also mentioned. The fraction of spike epitopes from Wu-1 strain that are fully conserved in each SARS-CoV-2 variant is listed. The logograms show

the conservation of all spike-derived T cell epitopes tested in this study for **(D)** HLA-A*02:01 **(E)** HLA-B*40:01 and **(F)** HLA-DRB1*15:01. The mutated residues are colored and labeled accordingly. An amino acid deletion is marked as ”-”.

Acknowledgements

We thank all the volunteers and patients for their participation in this study. We thank the Stanford Occupational Health staff and the Sean N. Parker Center for Allergy and Asthma Research staff for enrolling volunteers. We thank members from the laboratories of Mark Davis and Yueh-Hsiu Chien for helpful discussions. Flow cytometry analysis for this project was done on instruments in the Stanford Shared FACS Facility. HLA-typing was performed at the Stanford Functional Genomics Facility.

Funding

This work was supported by grants from the Howard Hughes Medical Institute and NIAID grant AI057229 to MMD. Additional support was provided by the Bill and Melinda Gates Foundation to MMD and VM (OPP1113682, Center for Human Systems Immunology. Further funds were provided by the Sean N Parker Center, the Sunshine Foundation, and U01 AI140498 to MM and KCN.

Author contributions

Project conceptualization and study design was performed by FG, VM and MMD. Experiments were performed by FG. Data analyses was performed by FG and VM. PSA, KvdP, MM, FY, OW, RH, EH, J-yL, CL, ASL, MMS, SBS, JG assisted with PBMC sample collection, processing and banking. KRK assisted with epitope selection. RW, VR and JDA provided MHC monomers. JL assisted with cell staining. KR performed antibody measurements with the supervision of SDB. TTW and BP provided resources for sample processing. PJ and KCN supervised volunteer recruitment. FG, VM and MMD wrote the manuscript with input from all the authors.

Declaration of interests

VM and MMD are inventors on a patent application (PCT/US2021/064378) on the spheromer technology described in this work. The other authors declare that they have no competing interests.

Inclusion and diversity

We support inclusive, diverse, and equitable conduct of research.

References

1. Chakraborty, S., Mallajosyula, V., Tato, C.M., Tan, G.S., and Wang, T.T. (2021). SARS-CoV-2 vaccines in advanced clinical trials: Where do we stand? Adv Drug Deliv Rev *172*, 314-338. 10.1016/j.addr.2021.01.014.
2. Polack, F.P., Thomas, S.J., Kitchin, N., Absalon, J., Gurtman, A., Lockhart, S., Perez, J.L., Perez Marc, G., Moreira, E.D., Zerbini, C., et al. (2020). Safety and Efficacy of the

BNT162b2 mRNA Covid-19 Vaccine. N Engl J Med *383*, 2603-2615. 10.1056/NEJMoa2034577.

3. Arunachalam, P.S., Scott, M.K.D., Hagan, T., Li, C., Feng, Y., Wimmers, F., Grigoryan, L., Trisal, M., Edara, V.V., Lai, L., et al. (2021). Systems vaccinology of the BNT162b2 mRNA vaccine in humans. Nature *596*, 410-416. 10.1038/s41586-021-03791-x.
4. Goel, R.R., Painter, M.M., Apostolidis, S.A., Mathew, D., Meng, W., Rosenfeld, A.M., Lundgreen, K.A., Reynaldi, A., Khoury, D.S., Pattekar, A., et al. (2021). mRNA vaccines induce durable immune memory to SARS-CoV-2 and variants of concern. Science *374*, abm0829. 10.1126/science.abm0829.
5. Roltgen, K., Nielsen, S.C.A., Silva, O., Younes, S.F., Zaslavsky, M., Costales, C., Yang, F., Wirz, O.F., Solis, D., Hoh, R.A., et al. (2022). Immune imprinting, breadth of variant recognition, and germinal center response in human SARS-CoV-2 infection and vaccination. Cell *185*, 1025-1040 e1014. 10.1016/j.cell.2022.01.018.
6. Sahin, U., Muik, A., Vogler, I., Derhovanessian, E., Kranz, L.M., Vormehr, M., Quandt, J., Bidmon, N., Ulges, A., Baum, A., et al. (2021). BNT162b2 vaccine induces neutralizing antibodies and poly-specific T cells in humans. Nature *595*, 572-577. 10.1038/s41586-021-03653-6.
7. Sievers, B.L., Chakraborty, S., Xue, Y., Gelbart, T., Gonzalez, J.C., Cassidy, A.G., Golan, Y., Prahl, M., Gaw, S.L., Arunachalam, P.S., et al. (2022). Antibodies elicited by SARS-CoV-2 infection or mRNA vaccines have reduced neutralizing activity against Beta and Omicron pseudoviruses. Sci Transl Med *14*, eabn7842. 10.1126/scitranslmed.abn7842.
8. Zhang, Z., Mateus, J., Coelho, C.H., Dan, J.M., Moderbacher, C.R., Galvez, R.I., Cortes, F.H., Grifoni, A., Tarke, A., Chang, J., et al. (2022). Humoral and cellular immune memory to four COVID-19 vaccines. bioRxiv. 10.1101/2022.03.18.484953.
9. Minervina, A.A., Pogorelyy, M.V., Kirk, A.M., Crawford, J.C., Allen, E.K., Chou, C.H., Mettelman, R.C., Allison, K.J., Lin, C.Y., Brice, D.C., et al. (2022). SARS-CoV-2 antigen exposure history shapes phenotypes and specificity of memory CD8(+) T cells. Nat Immunol *23*, 781-790. 10.1038/s41590-022-01184-4.
10. Mudd, P.A., Minervina, A.A., Pogorelyy, M.V., Turner, J.S., Kim, W., Kalaidina, E., Petersen, J., Schmitz, A.J., Lei, T., Haile, A., et al. (2022). SARS-CoV-2 mRNA vaccination elicits a robust and persistent T follicular helper cell response in humans. Cell *185*, 603-613 e615. 10.1016/j.cell.2021.12.026.
11. Oberhardt, V., Luxenburger, H., Kemming, J., Schulien, I., Ciminski, K., Giese, S., Csernalabics, B., Lang-Meli, J., Janowska, I., Staniek, J., et al. (2021). Rapid and stable mobilization of CD8(+) T cells by SARS-CoV-2 mRNA vaccine. Nature *597*, 268-273. 10.1038/s41586-021-03841-4.
12. Wragg, K.M., Lee, W.S., Koutsakos, M., Tan, H.X., Amarasena, T., Reynaldi, A., Gare, G., Konstandopoulos, P., Field, K.R., Esterbauer, R., et al. (2022). Establishment and recall of SARS-CoV-2 spike epitope-specific CD4(+) T cell memory. Nat Immunol *23*, 768-780. 10.1038/s41590-022-01175-5.
13. McMahan, K., Yu, J., Mercado, N.B., Loos, C., Tostanoski, L.H., Chandrashekar, A., Liu, J., Peter, L., Atyeo, C., Zhu, A., et al. (2021). Correlates of protection against SARS-CoV-2 in rhesus macaques. Nature *590*, 630-634. 10.1038/s41586-020-03041-6.

14. Berger, T., and Kornek, B. (2021). T cells step up after SARS-CoV-2 vaccination with B cell depletion. Nat Rev Neurol *17*, 729-730. 10.1038/s41582-021-00582-w.
15. Mallajosyula, V., Ganjavi, C., Chakraborty, S., McSween, A.M., Pavlovitch-Bedzyk, A.J., Wilhelmy, J., Nau, A., Manohar, M., Nadeau, K.C., and Davis, M.M. (2021). CD8(+) T cells specific for conserved coronavirus epitopes correlate with milder disease in COVID-19 patients. Sci Immunol *6*. 10.1126/sciimmunol.abg5669.
16. Swadling, L., Diniz, M.O., Schmidt, N.M., Amin, O.E., Chandran, A., Shaw, E., Pade, C., Gibbons, J.M., Le Bert, N., Tan, A.T., et al. (2022). Pre-existing polymerase-specific T cells expand in abortive seronegative SARS-CoV-2. Nature *601*, 110-117. 10.1038/s41586-021-04186-8.
17. Kosor Krnic, E., Gagro, A., Drazenovic, V., Kuzman, I., Jeren, T., Cecuk-Jelicic, E., Kerhin-Brkljacic, V., Gjenero-Margan, I., Kaic, B., Rakusic, S., et al. (2008). Enumeration of haemagglutinin-specific CD8+ T cells after influenza vaccination using MHC class I peptide tetramers. Scand J Immunol *67*, 86-94. 10.1111/j.1365-3083.2007.02042.x.
18. Su, L.F., Kidd, B.A., Han, A., Kotzin, J.J., and Davis, M.M. (2013). Virus-specific CD4(+) memory-phenotype T cells are abundant in unexposed adults. Immunity *38*, 373-383. 10.1016/j.immuni.2012.10.021.
19. Wild, K., Smits, M., Killmer, S., Strohmeier, S., Neumann-Haefelin, C., Bengsch, B., Krammer, F., Schwemmle, M., Hofmann, M., Thimme, R., et al. (2021). Pre-existing immunity and vaccine history determine hemagglutinin-specific CD4 T cell and IgG response following seasonal influenza vaccination. Nat Commun *12*, 6720. 10.1038/s41467-021-27064-3.
20. Han, A., Newell, E.W., Glanville, J., Fernandez-Becker, N., Khosla, C., Chien, Y.H., and Davis, M.M. (2013). Dietary gluten triggers concomitant activation of CD4+ and CD8+ alphabeta T cells and gammadelta T cells in celiac disease. Proc Natl Acad Sci U S A *110*, 13073-13078. 10.1073/pnas.1311861110.
21. Jagannathan, P., Andrews, J.R., Bonilla, H., Hedlin, H., Jacobson, K.B., Balasubramanian, V., Purington, N., Kamble, S., de Vries, C.R., Quintero, O., et al. (2021). Peginterferon Lambda-1a for treatment of outpatients with uncomplicated COVID-19: a randomized placebo-controlled trial. Nat Commun *12*, 1967. 10.1038/s41467-021-22177-1.
22. van der Ploeg, K., Kirosingh, A.S., Mori, D.A.M., Chakraborty, S., Hu, Z., Sievers, B.L., Jacobson, K.B., Bonilla, H., Parsonnet, J., Andrews, J.R., et al. (2022). TNF-alpha(+) CD4(+) T cells dominate the SARS-CoV-2 specific T cell response in COVID-19 outpatients and are associated with durable antibodies. Cell Rep Med *3*, 100640. 10.1016/j.xcrm.2022.100640.
23. Lopez Angel, C.J., Pham, E.A., Du, H., Vallania, F., Fram, B.J., Perez, K., Nguyen, T., Rosenberg-Hasson, Y., Ahmed, A., Dekker, C.L., et al. (2021). Signatures of immune dysfunction in HIV and HCV infection share features with chronic inflammation in aging and persist after viral reduction or elimination. Proc Natl Acad Sci U S A *118*. 10.1073/pnas.2022928118.
24. Ahmed, S.F., Quadeer, A.A., and McKay, M.R. (2020). Preliminary Identification of Potential Vaccine Targets for the COVID-19 Coronavirus (SARS-CoV-2) Based on SARS-CoV Immunological Studies. Viruses *12*. 10.3390/v12030254.

25. Gao, A., Chen, Z., Amitai, A., Doelger, J., Mallajosyula, V., Sundquist, E., Pereyra Segal, F., Carrington, M., Davis, M.M., Streeck, H., et al. (2021). Learning from HIV-1 to predict the immunogenicity of T cell epitopes in SARS-CoV-2. iScience *24*, 102311. 10.1016/j.isci.2021.102311.
26. Grifoni, A., Sidney, J., Vita, R., Peters, B., Crotty, S., Weiskopf, D., and Sette, A. (2021). SARS-CoV-2 human T cell epitopes: Adaptive immune response against COVID-19. Cell Host Microbe *29*, 1076-1092. 10.1016/j.chom.2021.05.010.
27. Prachar, M., Justesen, S., Steen-Jensen, D.B., Thorgrimsen, S., Jurgons, E., Winther, O., and Bagger, F.O. (2020). Identification and validation of 174 COVID-19 vaccine candidate epitopes reveals low performance of common epitope prediction tools. Sci Rep *10*, 20465. 10.1038/s41598-020-77466-4.
28. Chen, B., Khodadoust, M.S., Olsson, N., Wagar, L.E., Fast, E., Liu, C.L., Muftuoglu, Y., Sworder, B.J., Diehn, M., Levy, R., et al. (2019). Predicting HLA class II antigen presentation through integrated deep learning. Nat Biotechnol *37*, 1332-1343. 10.1038/s41587-019-0280-2.
29. Kim, Y., Ponomarenko, J., Zhu, Z., Tamang, D., Wang, P., Greenbaum, J., Lundegaard, C., Sette, A., Lund, O., Bourne, P.E., et al. (2012). Immune epitope database analysis resource. Nucleic Acids Res *40*, W525-530. 10.1093/nar/gks438.
30. Rammensee, H., Bachmann, J., Emmerich, N.P., Bachor, O.A., and Stevanovic, S. (1999). SYFPEITHI: database for MHC ligands and peptide motifs. Immunogenetics *50*, 213-219. 10.1007/s002510050595.
31. Newell, E.W., Klein, L.O., Yu, W., and Davis, M.M. (2009). Simultaneous detection of many T-cell specificities using combinatorial tetramer staining. Nat Methods *6*, 497-499. 10.1038/nmeth.1344.
32. Bettini, E., and Locci, M. (2021). SARS-CoV-2 mRNA Vaccines: Immunological Mechanism and Beyond. Vaccines (Basel) *9*. 10.3390/vaccines9020147.
33. Huang, H., Wang, C., Rubelt, F., Scriba, T.J., and Davis, M.M. (2020). Analyzing the Mycobacterium tuberculosis immune response by T-cell receptor clustering with GLIPH2 and genome-wide antigen screening. Nat Biotechnol *38*, 1194-1202. 10.1038/s41587-020-0505-4.
34. Tang, J., Zeng, C., Cox, T.M., Li, C., Son, Y.M., Cheon, I.S., Wu, Y., Behl, S., Taylor, J.J., Chakaraborty, R., et al. (2022). Respiratory mucosal immunity against SARS-CoV-2 after mRNA vaccination. Sci Immunol *7*, eadd4853. 10.1126/sciimmunol.add4853.
35. Arshad, N., Laurent-Rolle, M., Ahmed, W.S., Hsu, J.C., Mitchell, S.M., Pawlak, J., Sengupta, D., Biswas, K.H., and Cresswell, P. (2023). SARS-CoV-2 accessory proteins ORF7a and ORF3a use distinct mechanisms to down-regulate MHC-I surface expression. Proc Natl Acad Sci U S A *120*, e2208525120. 10.1073/pnas.2208525120.
36. Moriyama, M., Lucas, C., Monteiro, V.S., Yale, S.-C.-G.S.I., and Iwasaki, A. (2022). SARS-CoV-2 Omicron subvariants evolved to promote further escape from MHC-I recognition. bioRxiv. 10.1101/2022.05.04.490614.
37. Yoo, J.S., Sasaki, M., Cho, S.X., Kasuga, Y., Zhu, B., Ouda, R., Orba, Y., de Figueiredo, P., Sawa, H., and Kobayashi, K.S. (2021). SARS-CoV-2 inhibits induction of the MHC class I pathway by targeting the STAT1-IRF1-NLRC5 axis. Nat Commun *12*, 6602. 10.1038/s41467-021-26910-8.

38. Lozano-Ojalvo, D., Camara, C., Lopez-Granados, E., Nozal, P., Del Pino-Molina, L., Bravo-Gallego, L.Y., Paz-Artal, E., Pion, M., Correa-Rocha, R., Ortiz, A., et al. (2021). Differential effects of the second SARS-CoV-2 mRNA vaccine dose on T cell immunity in naive and COVID-19 recovered individuals. Cell Rep *36*, 109570. 10.1016/j.celrep.2021.109570.
39. Tarke, A., Coelho, C.H., Zhang, Z., Dan, J.M., Yu, E.D., Methot, N., Bloom, N.I., Goodwin, B., Phillips, E., Mallal, S., et al. (2022). SARS-CoV-2 vaccination induces immunological T cell memory able to cross-recognize variants from Alpha to Omicron. Cell *185*, 847-859 e811. 10.1016/j.cell.2022.01.015.
40. Hachmann, N.P., Miller, J., Collier, A.Y., Ventura, J.D., Yu, J., Rowe, M., Bondzie, E.A., Powers, O., Surve, N., Hall, K., and Barouch, D.H. (2022). Neutralization Escape by SARS-CoV-2 Omicron Subvariants BA.2.12.1, BA.4, and BA.5. N Engl J Med. 10.1056/NEJMc2206576.
41. Wang, Q., Iketani, S., Li, Z., Liu, L., Guo, Y., Huang, Y., Bowen, A.D., Liu, M., Wang, M., Yu, J., et al. (2022). Alarming antibody evasion properties of rising SARS-CoV-2 BQ and XBB subvariants. Cell. 10.1016/j.cell.2022.12.018.
42. Poon, L., Gu, H., Quadeer, A.A., Krishnan, P., Chang, L., Liu, G., Ng, D., Cheng, S., Lam, T.T., Peiris, M., and McKay, M. (2022). Within-host diversity of SARS-CoV-2 lineages and effect of vaccination. Res Sq. 10.21203/rs.3.rs-1927944/v1.
43. Antonio, E.C., Meireles, M.R., Bragatte, M.A.S., and Vieira, G.F. (2022). Viral immunogenic footprints conferring T cell cross-protection to SARS-CoV-2 and its variants. Front Immunol *13*, 931372. 10.3389/fimmu.2022.931372.
44. Sidhom, J.-W., and Baras, A.S. (2020). Analysis of SARS-CoV-2 specific T-cell receptors in ImmuneCode reveals cross-reactivity to immunodominant Influenza M1 epitope. bioRxiv.
45. Bergamaschi, C., Terpos, E., Rosati, M., Angel, M., Bear, J., Stellas, D., Karaliota, S., Apostolakou, F., Bagratuni, T., Patseas, D., et al. (2021). Systemic IL-15, IFN-gamma, and IP-10/CXCL10 signature associated with effective immune response to SARS-CoV-2 in BNT162b2 mRNA vaccine recipients. Cell Rep *36*, 109504. 10.1016/j.celrep.2021.109504.
46. Chakraborty, S., Gonzalez, J.C., Sievers, B.L., Mallajosyula, V., Chakraborty, S., Dubey, M., Ashraf, U., Cheng, B.Y., Kathale, N., Tran, K.Q.T., et al. (2022). Early non-neutralizing, afucosylated antibody responses are associated with COVID-19 severity. Sci Transl Med *14*, eabm7853. 10.1126/scitranslmed.abm7853.
47. Wang, D., Hu, B., Hu, C., Zhu, F., Liu, X., Zhang, J., Wang, B., Xiang, H., Cheng, Z., Xiong, Y., et al. (2020). Clinical Characteristics of 138 Hospitalized Patients With 2019 Novel Coronavirus-Infected Pneumonia in Wuhan, China. JAMA *323*, 1061-1069. 10.1001/jama.2020.1585.
48. Ma, M.J., Qiu, S.F., Cui, X.M., Ni, M., Liu, H.J., Ye, R.Z., Yao, L., Liu, H.B., Cao, W.C., and Song, H.B. (2022). Persistent SARS-CoV-2 infection in asymptomatic young adults. Signal Transduct Target Ther *7*, 77. 10.1038/s41392-022-00931-1.
49. Eggink, D., Andeweg, S.P., Vennema, H., van Maarseveen, N., Vermaas, K., Vlaemynck, B., Schepers, R., van Gageldonk-Lafeber, A.B., van den Hof, S., Reusken, C.B., and Knol, M.J. (2022). Increased risk of infection with SARS-CoV-2 Omicron BA.1 compared with Delta in vaccinated and previously infected individuals, the Netherlands, 22 November 2021 to 19 January 2022. Euro Surveill *27*. 10.2807/1560-7917.ES.2022.27.4.2101196.

50. Chin, E.T., Leidner, D., Lamson, L., Lucas, K., Studdert, D.M., Goldhaber-Fiebert, J.D., Andrews, J.R., and Salomon, J.A. (2022). Protection against Omicron from Vaccination and Previous Infection in a Prison System. N Engl J Med *387*, 1770-1782. 10.1056/NEJMoa2207082.
51. Altarawneh, H.N., Chemaitelly, H., Ayoub, H.H., Tang, P., Hasan, M.R., Yassine, H.M., Al-Khatib, H.A., Smatti, M.K., Coyle, P., Al-Kanaani, Z., et al. (2022). Effects of Previous Infection and Vaccination on Symptomatic Omicron Infections. N Engl J Med *387*, 21-34. 10.1056/NEJMoa2203965.
52. Apostolidis, S.A., Kakara, M., Painter, M.M., Goel, R.R., Mathew, D., Lenzi, K., Rezk, A., Patterson, K.R., Espinoza, D.A., Kadri, J.C., et al. (2021). Cellular and humoral immune responses following SARS-CoV-2 mRNA vaccination in patients with multiple sclerosis on anti-CD20 therapy. Nat Med *27*, 1990-2001. 10.1038/s41591-021-01507-2.
53. Oh, B.L.Z., Tan, N., de Alwis, R., Kunasegaran, K., Chen, Z., Poon, M., Chan, E., Low, J.G.H., Yeoh, A.E.J., Bertoletti, A., and Le Bert, N. (2022). Enhanced BNT162b2 vaccine-induced cellular immunity in anti-CD19 CAR T cell-treated patients. Blood *140*, 156-160. 10.1182/blood.2022016166.
54. Toebes, M., Rodenko, B., Ovaa, H., and Schumacher, T.N. (2009). Generation of peptide MHC class I monomers and multimers through ligand exchange. Curr Protoc Immunol *Chapter 18*, Unit 18 16. 10.1002/0471142735.im1816s87.
55. Willis, R.A., Ramachandiran, V., Shires, J.C., Bai, G., Jeter, K., Bell, D.L., Han, L., Kazarian, T., Ugwu, K.C., Laur, O., et al. (2021). Production of Class II MHC Proteins in Lentiviral Vector-Transduced HEK-293T Cells for Tetramer Staining Reagents. Curr Protoc *1*, e36. 10.1002/cpz1.36.

STAR Methods

Resource availability

Lead Contact

Further information and requests for resources and reagents should be directed to and will be fulfilled by the lead contact, Mark. M. Davis (mmdavis@stanford.edu).

Materials availability

Upon specific request and execution of a material transfer agreement (MTA) from School of Medicine, Stanford University to the Lead Contact, the peptide-MHC spheromer reagents will be made available.

Data and code availability

The data supporting the findings of this study are available within the published article and summarized in the corresponding tables, figures, and supplemental materials. Any additional information required to reanalyze the data reported in this paper is available from the lead contact upon request.

Experimental model and subject details

Human blood sample collection

The BNT162b2 vaccine donors were recruited for the study with informed consent. The study was approved by the Stanford University Institutional Review Board (IRB 8629) and was conducted with full compliance of Good Clinical Practice as per the Code of Federal Regulations. Part of the COVID-19 patient peripheral blood mononuclear cells (PBMCs) sample collection for this study was done at the Stanford Occupational Health under an IRB approved protocol (Protocol Director, Kari C. Nadeau). We obtained samples from adults who had a positive test result for the SARS-CoV-2 virus from an analysis of their nasopharyngeal swab specimens obtained at any point from March 2020 - June 2020. Stanford Health Care clinical laboratory developed internal testing capability with a reverse-transcriptase based polymerase-chain-reaction assay (RT-PCR). All participants consented prior to enrolling in the study. The other COVID-19 patient samples used were from 109 participants enrolled in a Phase 2, single-blind, randomized placebo-controlled trial evaluating the efficacy of Peginterferon Lambda-1a in SARS-CoV-2 infected outpatients[21,22]. The trial was registered at ClinicalTrials.gov (NCT04331899) and was performed as an investigator-initiated clinical trial with the FDA (IND 419217). In brief, symptomatic outpatients aged 18–71 who tested positive for reverse transcription-polymerase chain reaction (RT-PCR) detection of SARS-CoV-2 within 72 h of enrollment were eligible to participate in the study barring any signs of respiratory distress. Asymptomatic patients were eligible if they had not previously had a positive SARS-CoV-2 test. Full eligibility and exclusion criteria are provided in the study protocol and have been published[21,22]. PBMC samples from healthy donors were obtained from the Stanford Blood Center according to our IRB approved protocol. All healthy donor samples used in

the current study were collected between April 2018 to Feb 2019 before the SARS-CoV-2 pandemic.

Method details

Assembly of pMHC-spheromers

A novel multimeric αβ T cell staining reagent, spheromer, that we reported recently was used to analyze the epitope-specific $CD8^+$ and $CD4^+$ T cell responses[15]. The MHC protein purification and peptide exchange were conducted as previously described[54,55]. The list of peptides used in this study are provided in Table S1. The peptides evaluated in our study were chosen based on a combination of the following criteria: literature search[6,9-12,15,24-27], bioinformatic analysis, and MHC stabilization assay. A total of 49 peptides across the entire SARS-CoV-2 genome (SARS-CoV-2/USA/WA-CDC-WA1/2020; Wu-1 strain) were profiled in this study. Briefly, a preliminary list was curated using a combination of previous studies[6,9-12,15,24-27] and predicted binding affinities using the immune epitope database and analysis resource (IEDB) recommendations (http://tools.iedb.org/)[29]. Peptides identified from a literature search were included for further analysis only if they were predicted as “strong” binders using the IEDB recommended allele-specific affinity cutoff (HLA-A*02:01 – 255nM and HLA-B*40:01 – 639nM). For HLA-DRB1*15:01, peptides were selected based on a consensus percentile rank of ≤10%. Next, we cross-validated these ‘hits’ using the SYFPEITHI[30] and MARIA[28] algorithms. MARIA is a deep learning-based algorithm that reportedly outperforms existing prediction methods. Furthermore, amino acids at anchor positions were given

higher weights. We also used an MHC stabilization assay to experimentally validate the binding of peptides to ectopically expressed MHC molecules in antigen processing (TAP)–deficient T2 cell lines. Accordingly, we built a broad panel of SARS-CoV-2 peptides (CD8 – spike = 14, non-spike = 24; CD4 – spike = 5, non-spike = 6) representing a wide range of sequence conservation across seasonal human coronaviruses. This enabled us to compare the epitope-specific response kinetics between infection and vaccination, and evaluate the contribution of pre-existing, cross-reactive T cells. The Pfizer/BioNTech BNT162b2 vaccine has two proline mutations (K986P and V987P) to stabilize the spike protein. The engineered maxi-ferritin scaffold was also purified as described previously[15] and used spheromer assembly. In brief, the assembly was performed in two steps: 1) Generation of a semi-saturated SAv-$pMHC_2$ complex, and 2) Conjugation of SAv-$pMHC_2$ to the functionalized maxi-ferritin scaffold. SAv-$pMHC_2$ was obtained by incubating 1 µM of the pMHC with 0.45 µM of SAv at 25°C for 30 min without agitation. Subsequently, the spheromer complex was assembled by incubating SAv-$pMHC_2$ with the functionalized scaffold for 1h at room temperature with mild rotation. The fluorophore-conjugated SAv was sourced from Invitrogen. For the simultaneous detection of multiple SARS-CoV-2 spike epitopes using the spheromer technology, we adapted a combinatorial staining approach developed previously[31]. Briefly, each peptide was assigned a unique fluorophore-barcode that allows the simultaneous detection of 2^n-1 specificities in a sample, where n is the number of distinct fluorophore labels. The relative concentrations for pMHC monomers associated with each fluorophore label was experimentally determined.

PBMC staining and flow cytometry

PBMCs were thawed in a water bath set at 37°C and the cells were immediately transferred to warm RPMI media (Thermo Fisher Scientific) supplemented with 10% FBS (R&D Systems) and 100U/ml of penicillin-streptomycin. After washing, the cells were filtered using a 70µm cell strainer and rested for 1h at 37°C. T cells were enriched from PBMCs by negative selection using a FITC-conjugated antibody cocktail including anti-CD14 (Clone HCD14, BioLegend), anti-CD19 (Clone HIB19, BioLegend), anti-CD33 (Clone HIM3-4, BioLegend) and anti-γδ TCR (Clone 5A6.E9, ThermoFisher Scientific) followed by magnetic bead depletion using anti-FITC microbeads (Miltenyi Biotec). The enriched T cells were washed and resuspended in FACS buffer for staining. All spheromer staining was done for 1h after incubating the cells with Human TruStain FcX (BioLegend) for 15 min on ice. The spheromer were used at a monomeric concentration of ~100nM and ~500nM for the staining of $CD8^+$ T cells and $CD4^+$ T cells, respectively. The cells were subsequently stained with anti-CD19 (BV510, clone HIB19), anti-γδTCR (BV510, clone B1), anti-CD33 (BV510, clone HIM3-4), anti-CD3 (PE/Cyanine7, clone OKT3), anti-CD8 (BUV396, clone RPA-T8, BD Biosciences), anti-CD4 (BV785, clone RPA-T4), anti-CCR7 (PE/Dazzle 594, clone G043H7), anti-CD45RA (BV711, clone HI100) and an amine-reactive viability stain (Live/dead fixable aqua dead cell stain kit; Invitrogen) for 30 min on ice, washed, resuspended in FACS buffer and acquired on a BD LSRII flow cytometer. The data was analyzed using FlowJo (v10) software.

Peptide mega pool (MP) and single peptide stimulation

Frozen PBMCs were thawed, counted, and resuspended at a density of 15 million live cells per ml in complete RPMI (RPMI with 10% FBS (Gibco) and antibiotics). 100 µl of cell suspension containing 1.5 million cells was added to each well of a 96-well round-bottomed tissue culture plate. The cells were rested overnight at 37 °C in a CO_2 incubator. The next morning, each sample was treated with peptide mega pool (1 µg/ml of each peptide) or single peptide (5 µg/ml) or 0.5% v/v DMSO as negative control in the presence of 1 µg/ml of anti-CD28 (clone CD28.2, BD Biosciences), anti-CD49d (clone 9F10, BD Biosciences), anti-CXCR3 (clone 1C6, BD Biosciences) and anti-CXCR5 (clone RF8B2, BD Biosciences). Peptides were synthesized to 95% purity (Elim Biopharm). All wells contained 0.5% v/v DMSO in total volume of 200 µl per well. The samples were incubated at 37 °C in CO_2 incubators for 2 h, and then 10 µg/ml brefeldin-A was added. The cells were further incubated for 6-8 h.

Intracellular cytokine staining (ICS) assay

After peptide stimulation, the cells were washed with PBS containing 5% FCS and stained with amine-reactive viability stain (Live/dead fixable aqua dead cell stain kit; Invitrogen) for 30 min at 4°C. After washing, pMHC-spheromers were added to screen the epitope-specific $CD8^+$ and $CD4^+$ T cells. The samples were stained for 30 min at 4°C in 100 µl volume. After spheromer staining, the cells were washed, fixed and permeabilized with cytofix/cytoperm buffer (BD Biosciences) for 20 min. The permeabilized cells were stained with ICS antibodies (anti-IL2 (clone MQ1-17H12, Biolegend), anti-TNFα (clone Mab11, BD Biosciences), anti-IFNγ (clone B27, BD Biosciences) and anti-GranZB (clone QA16A02, Biolegend)) for 20 min at room temperature in 1X perm/wash buffer (BD

997 Biosciences). Cells were then washed twice with perm/wash buffer and once with staining
998 buffer before acquisition using BD LSRII flow cytometer. The data was analyzed using
999 FlowJo (v10) software.
1000
1001 **Activation induced marker (AIM) assay**
1002 After peptide stimulation, the cells were washed with PBS containing 5% FCS and stained
1003 with amine-reactive viability stain (Live/dead fixable aqua dead cell stain kit; Invitrogen)
1004 for 30 min at 4°C. After washing, pMHC-spheromers were added to screen the epitope-
1005 specific $CD8^+$ and $CD4^+$ T cells. Meanwhile, the antibody cocktail was added for AIM
1006 staining (anti-CD69 (clone FN50, Biolegend), anti-CD154 (clone 24-31, Biolegend), anti-
1007 CD137 (clone 4B4-1, Biolegend), anti-CD38 (clone HIT2, BD Biosciences) and anti-Ki-67
1008 (clone B56, BD Biosciences)). The cells were stained for 30 min at 4°C in 100µl volume.
1009 Cells were then washed twice with staining buffer before acquisition using BD LSRII flow
1010 cytometer. The data was analyzed using FlowJo (v10) software.
1011
1012 **Quantification and statistical analysis**
1013 Statistical analysis was performed using GraphPad Prism 8, GraphPad Software, San
1014 Diego, California, USA. We performed a meta-analysis to combine the p-values from
1015 individual hypothesis tests to assess the significance of the overall distribution. Data were
1016 considered statistically significant when $p < 0.05$. Dimensionality reduction analysis were
1017 also performed in R. UMAP to visualize multiparametric flow cytometry data was
1018 generated using the “umap” package. The statistical details for each experiment are
1019 provided in the associated figure legends.

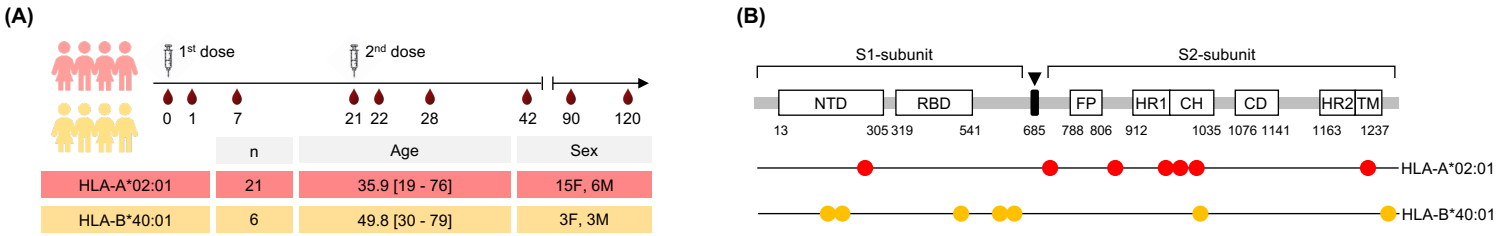

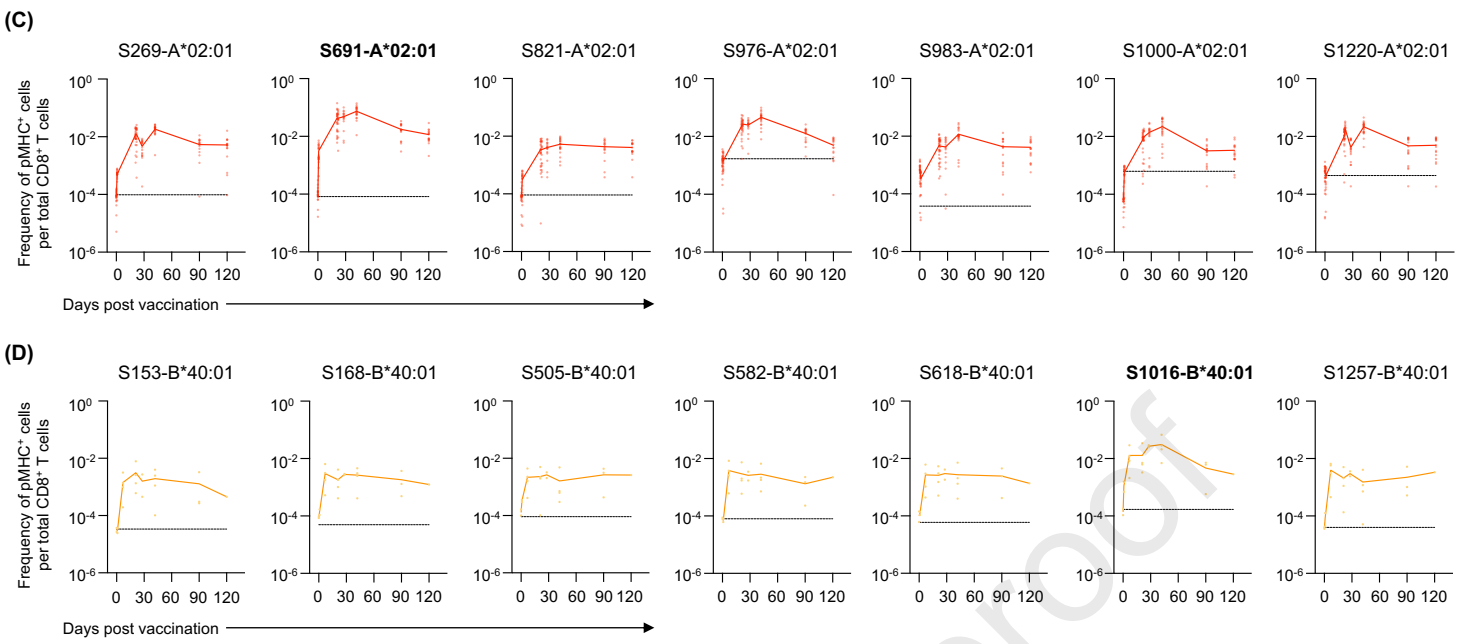

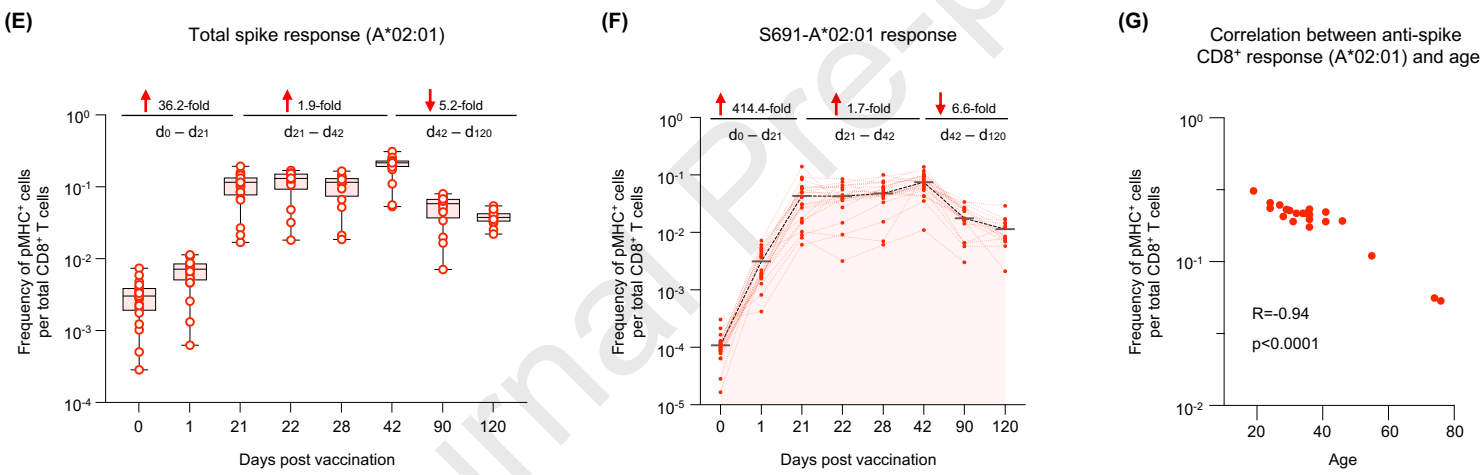

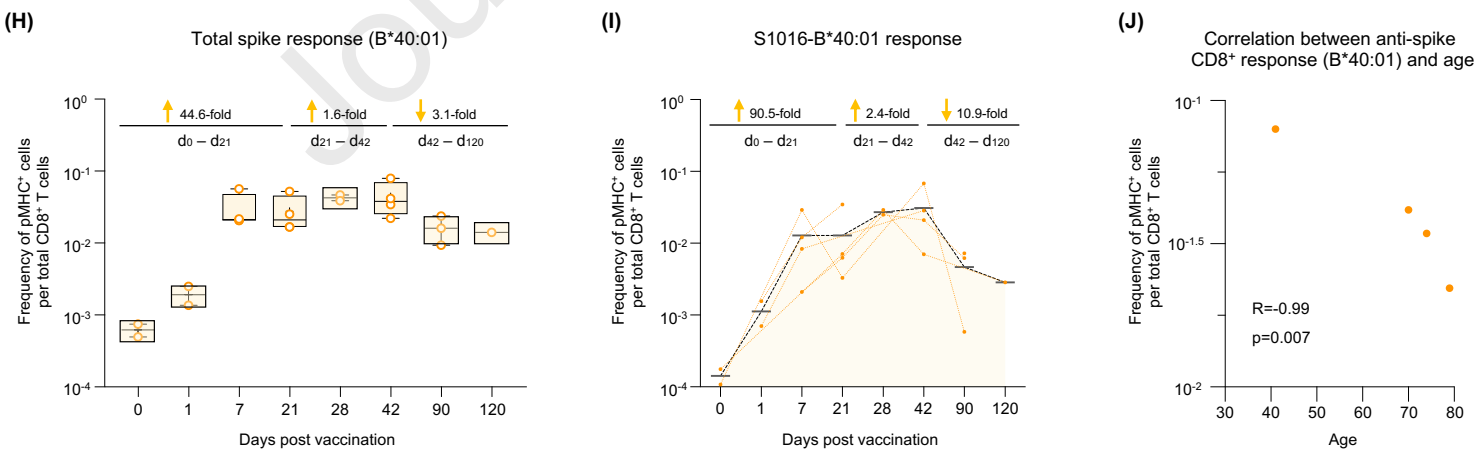

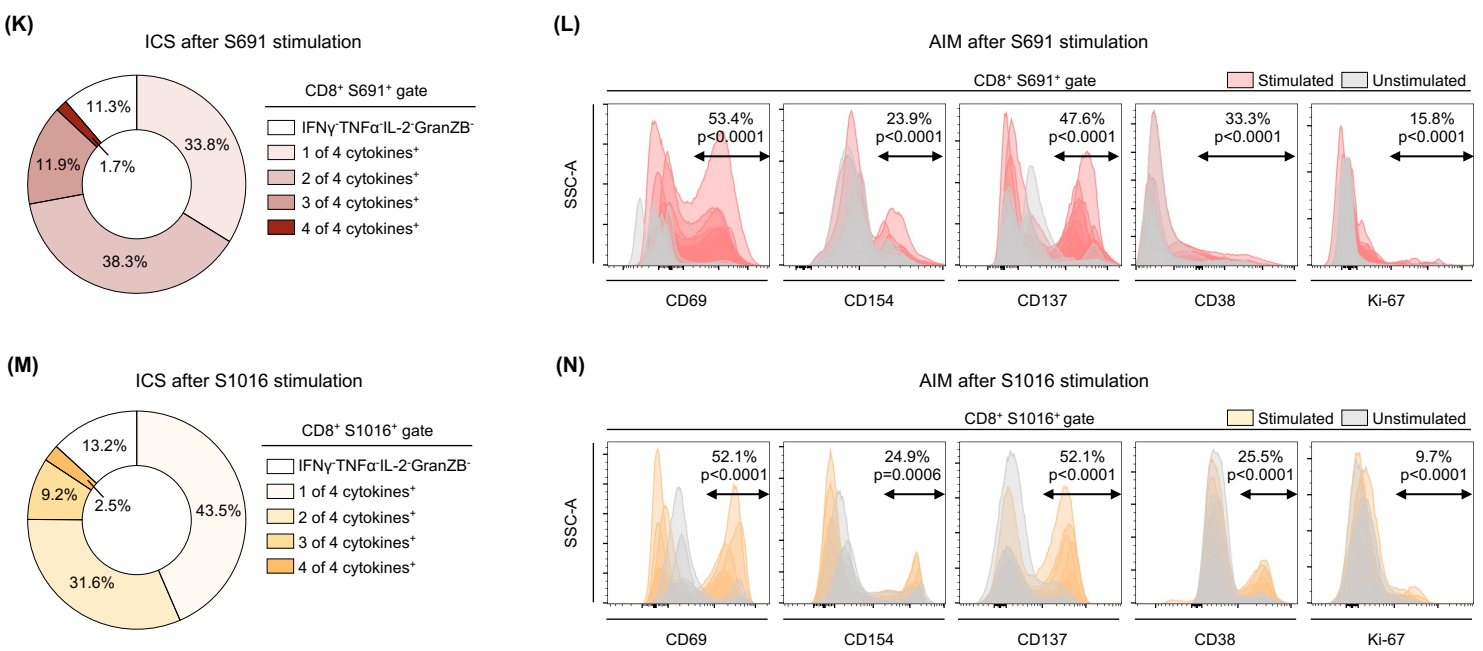

Figure 2

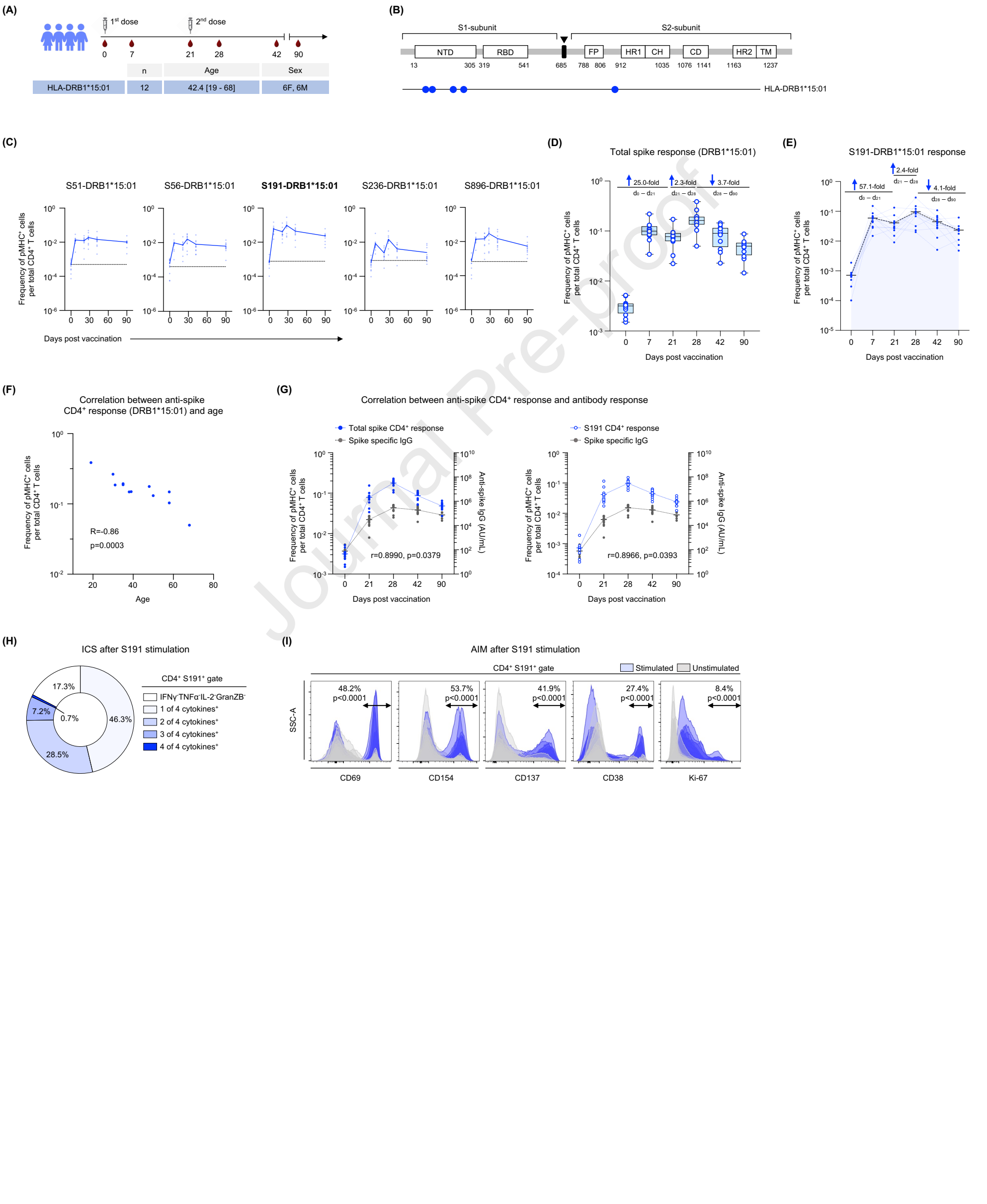

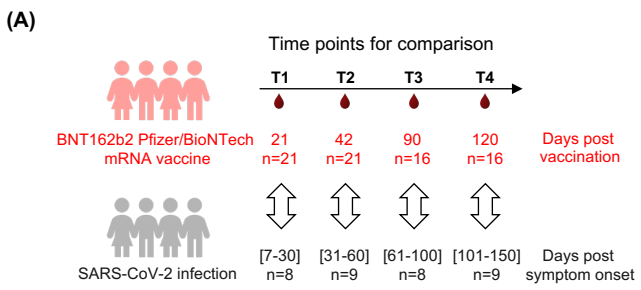

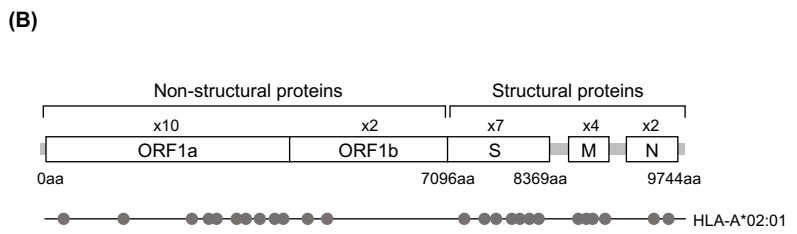

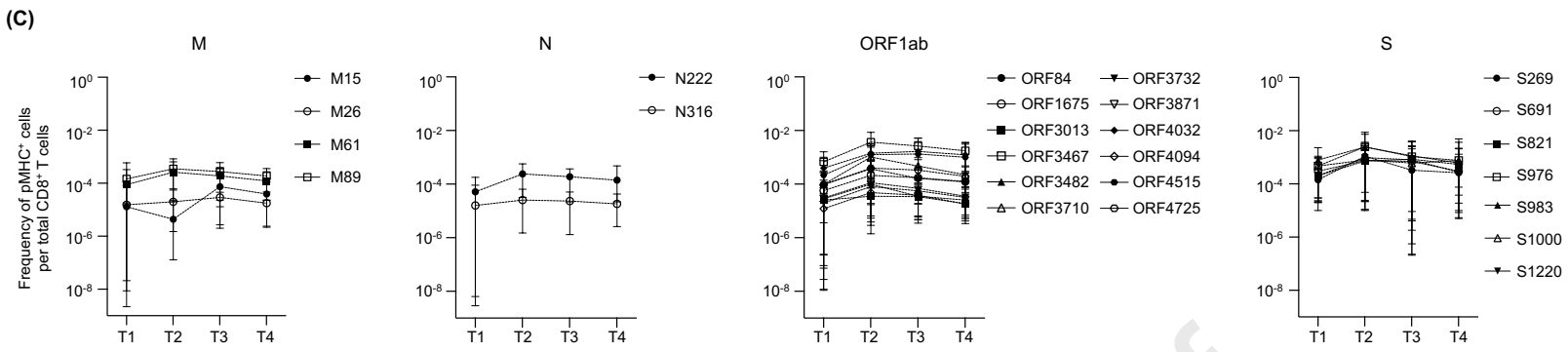

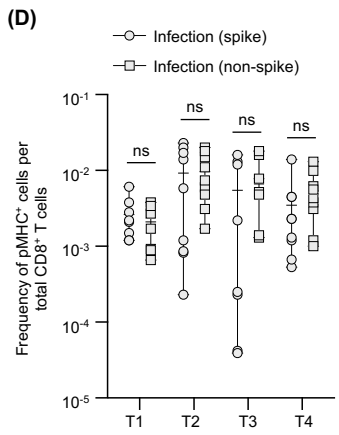

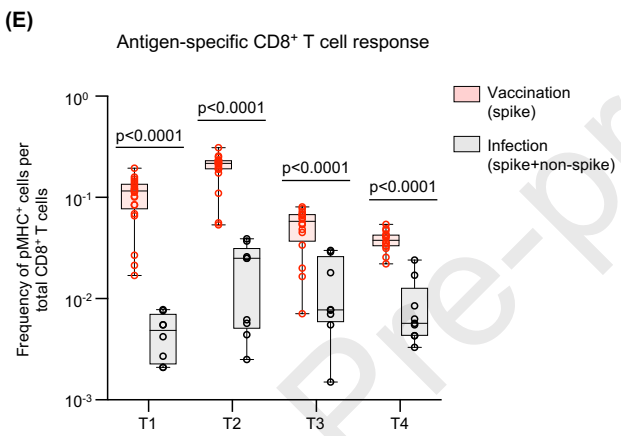

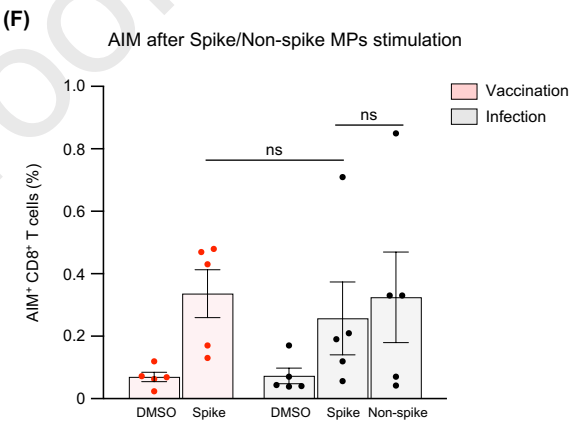

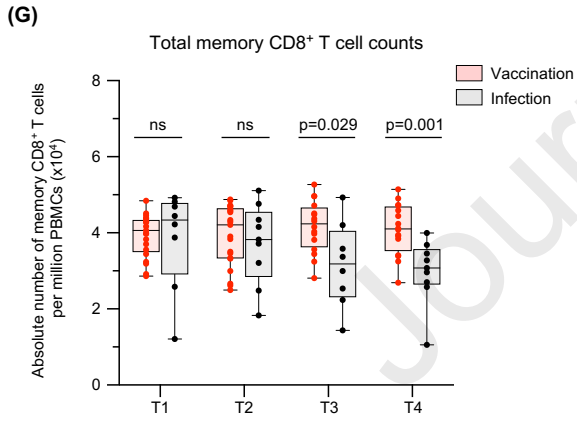

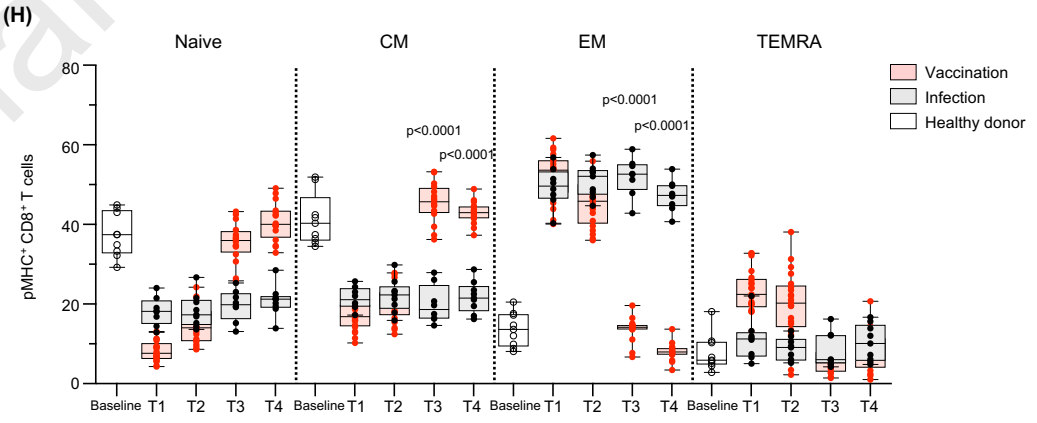

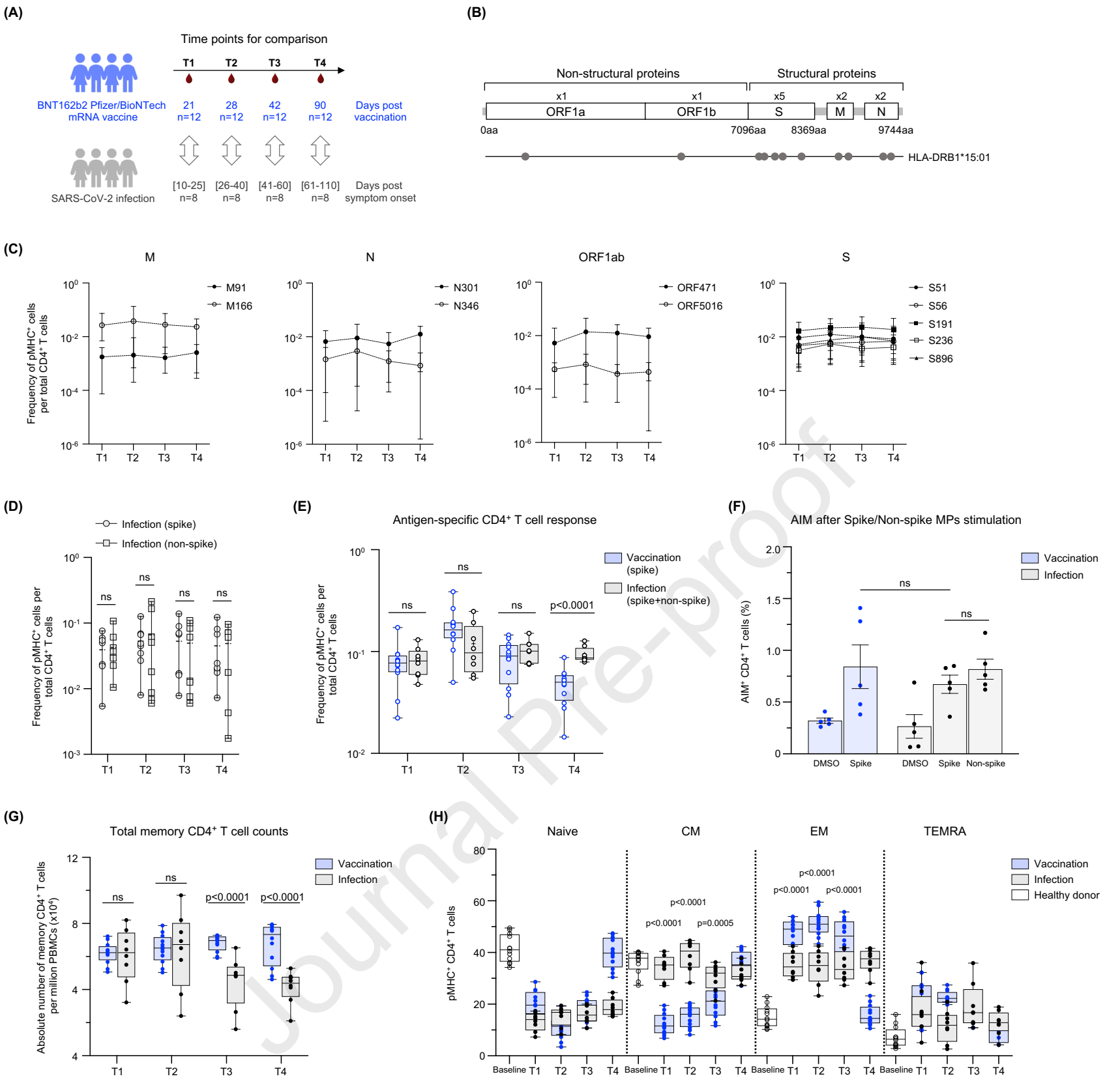

Figure 5

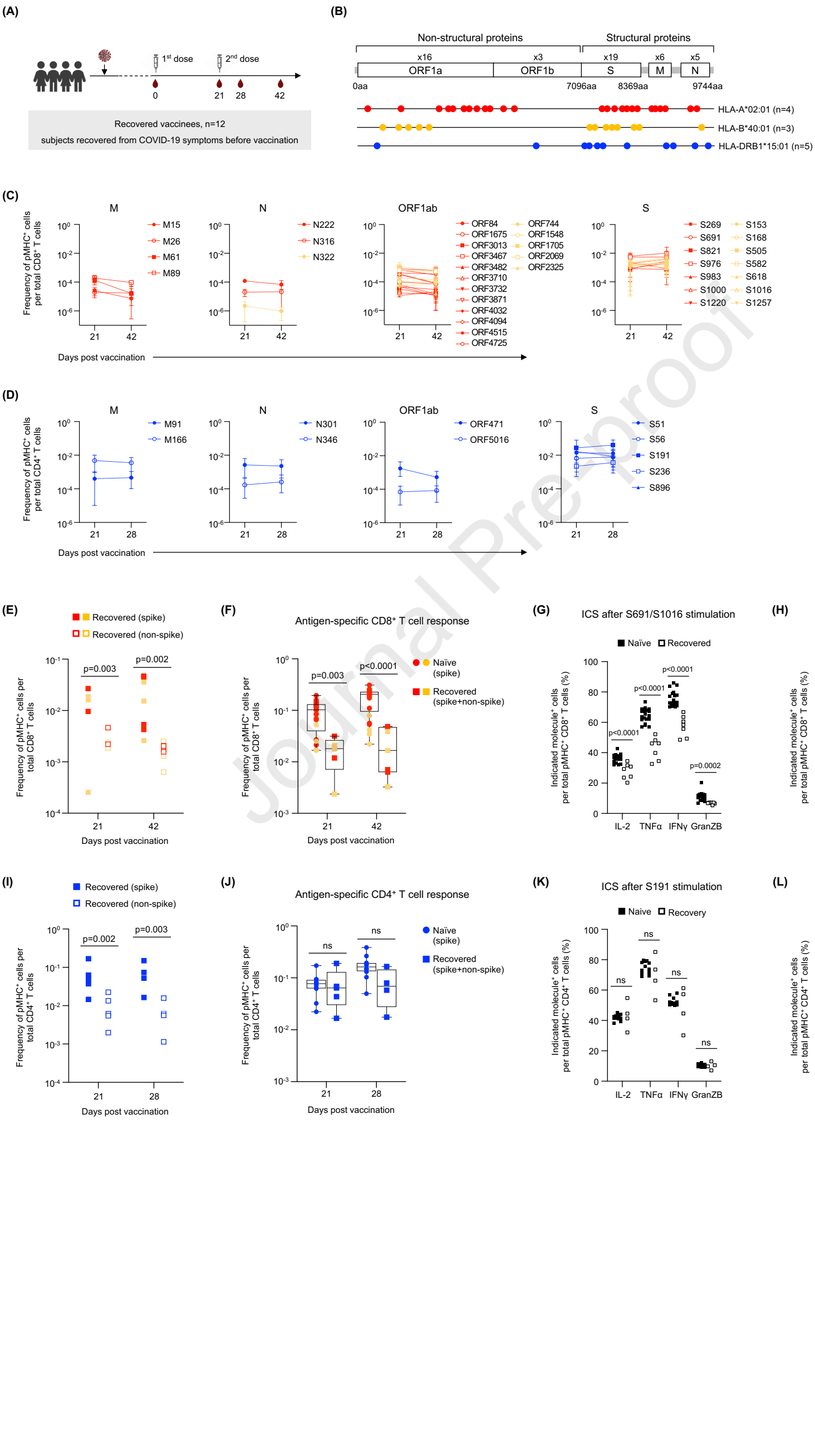

Figure 6

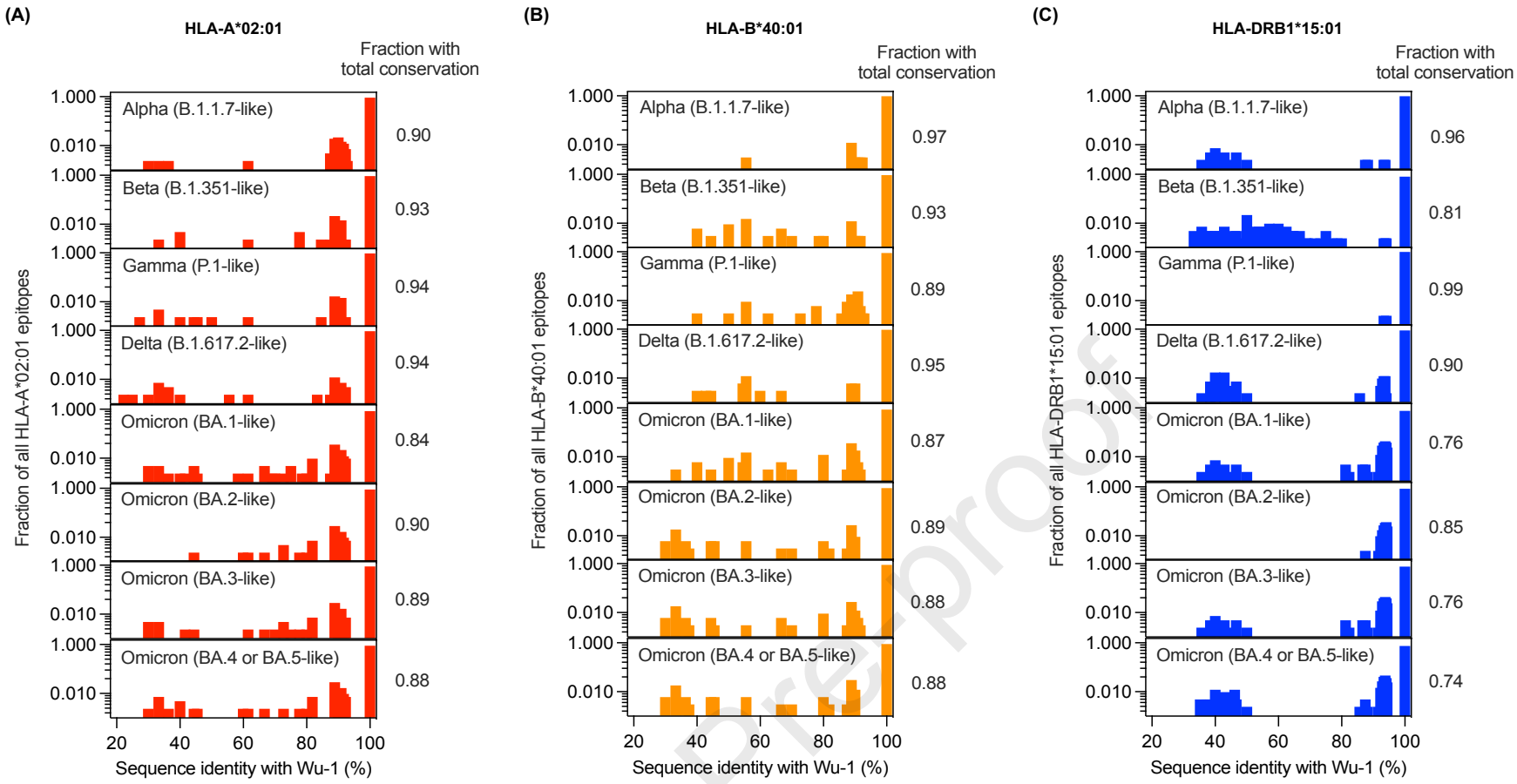

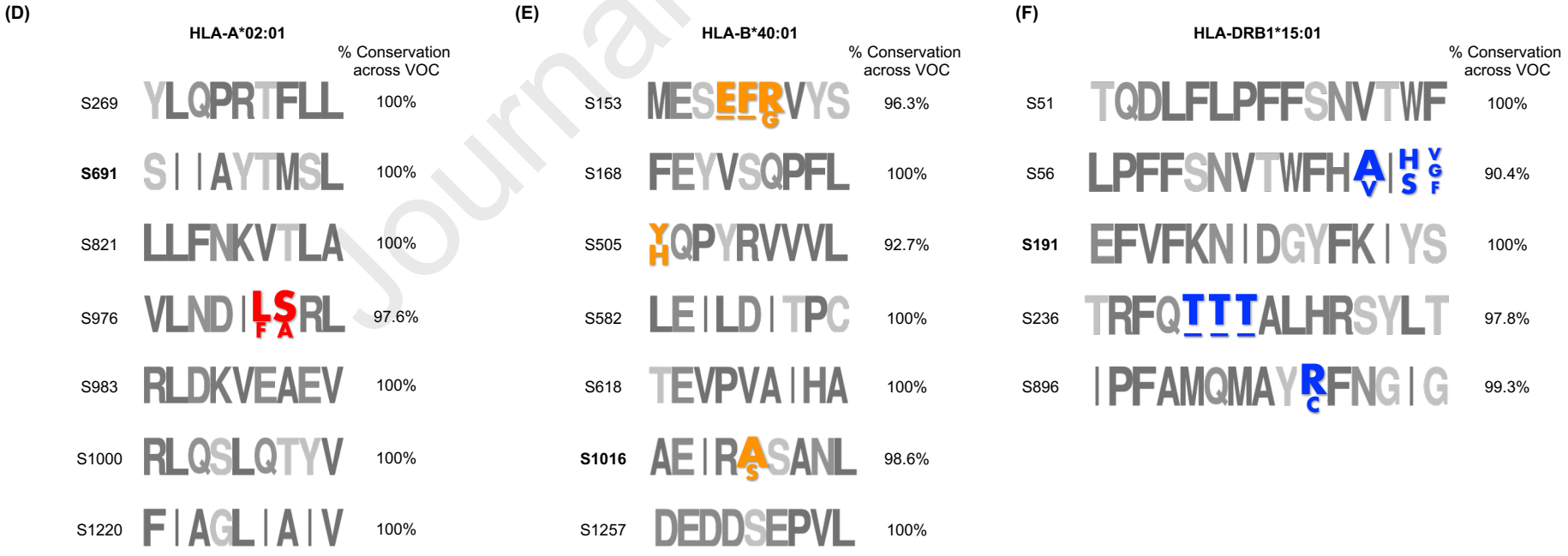

Highlights

- CD8+ and CD4+ T cell responses characterized using SARS-CoV-2 pMHC-spheromers.
- CD8+ and CD4+ T cell response kinetics are decoupled after mRNA vaccination.
- Reduced peripheral CD8+ T cell responses after infection compared to mRNA vaccination.
- Prior exposure limits peripheral CD8+ T cell responses after mRNA vaccination.

eTOC Blurb

Our understanding of T cell responses in COVID-19 and vaccination is incomplete. Gao et al. examine SARS-CoV-2-specific T cell responses to infection and vaccination, revealing disparate kinetics between CD4+ and CD8+ T cells. Furthermore, compared to vaccination alone, circulating CD8+ T cells are attenuated during infection and in subsequent vaccination.

Key resources table

REAGENT or RESOURCE	SOURCE	IDENTIFIER
Antibodies		
anti-CD14	BioLegend	Clone HCD14
anti-CD19	BioLegend	Clone HIB19
anti-CD33	BioLegend	Clone HIM3-4
anti-γδ TCR	Thermo Fisher Scientific	Clone 5A6.E9
anti-γδTCR	BioLegend	clone B1
anti-CD3	BioLegend	clone OKT3
anti-CD8	BD Biosciences	clone RPA-T8
anti-CD4	BD Biosciences	clone RPA-T4
anti-CCR7	BioLegend	clone G043H7
anti-CD45RA	BioLegend	clone HI100
anti-CD28	BD Biosciences	clone CD28.2
anti-CD49d	BD Biosciences	clone 9F10
anti-CXCR3	BD Biosciences	clone 1C6
anti-CXCR5	BD Biosciences	clone RF8B2
anti-IL2	Biolegend	clone MQ1-17H12
anti-TNFa	BD Biosciences	clone Mab11
anti-IFNg	BD Biosciences	clone B27
anti-GranZB	Biolegend	clone QA16A02
anti-CD69	Biolegend	clone FN50
anti-CD154	Biolegend	clone 24-31
anti-CD137	Biolegend	clone 4B4-1
anti-CD38	BD Biosciences	clone HIT2
anti-Ki-67	BD Biosciences	clone B56
Biological samples		
PBMC samples from BNT162b2 vaccine donors	Stanford Good Clinical Practice	IRB 8629
PBMC samples from COVID-19 patient	Stanford Occupational Health	IRB 55689 and IRB 55619
PBMC samples from COVID-19 recovered BNT162b2 vaccinated donors	Stanford Good Clinical Practice and Stanford Occupational Health	IRB 8629, IRB 55689, and IRB 55619
Chemicals, peptides, and recombinant proteins		
Human TruStain FcX	BioLegend	#422302
Benzonase nuclease	Millipore Sigma	#71206
MHC-I monomer	NIH tetramer facility core	HLA-A*02:01 and HLA-B*40:01
MHC-II monomer	NIH tetramer facility core	HLA-DRB1*15:01
Peptides (synthesized to 95% purity)	Elim Biopharm	Sequences shown in table S1
Streptavidin PE-Cyanine7 Conjugate	Thermo Fisher Scientific	# 25-4317-82
Streptavidin PE Conjugate	Thermo Fisher Scientific	#12-4317-87

Streptavidin eFluor™ 450 Conjugate	Thermo Fisher Scientific	#48-4317-82
Streptavidin Alexa Fluor™ 647 conjugate	Thermo Fisher Scientific	#S21374
Streptavidin Brilliant Violet 711 conjugate	BioLegend	#405241
Streptavidin Brilliant Violet 785 conjugate	BioLegend	#405249
Streptavidin PE/Dazzle 594 conjugate	BioLegend	#405247
Cytofix/cytoperm buffer	BD Biosciences	#554714
Perm/wash buffer	BD Biosciences	#554723
Brefeldin-A solution	Thermo Fisher Scientific	#00-4506-51
anti-FITC microbeads	Miltenyi Biotec	#130-048-701
Live/dead fixable aqua dead cell stain kit	Invitrogen	#L34957
Software and algorithms		
GraphPad Prism 8	GraphPad software	https://www.graphpad.com/scientificsoftware/prism/
UMAP code package	R studio	N/A
FlowJo 10	BD	https://www.flowjo.com/
IEDB	IEDB website	http://tools.iedb.org/)
SYFPEITHI	SYFPEITHI website	http://www.syfpeithi.de/
MARIA	MARIA Stanford	https://maria.stanford.edu/about.php
Other		
RPMI 1640 media	Thermo Fisher Scientific	#11875085
Fetal Bovine Serum	R&D Systems	S11150
FACS tube with 70-µm mesh cap	ThermoFisher Scientific	#08-771-23
30K Amicon tubes	Millipore	#UFC903024
70µm cell strainer	Corning	07-201-431
anti-FITC microbeads	Miltenyi Biotec	130-048-701
96-well plates	Corning	#3916

HLA-restriction	Protein	ID	SARS-CoV-2 sequence
HLA-A*02:01	M	M_15	KLLEQWNLV
		M_26	FLFLTWICL
		M_61	TLACFVLAA
		M_89	GLMWLSYFI
	N	N_222	LLLDRLNQL
		N_316	GMSRIGMEV
	ORF1ab	ORF1ab_84	VMVELVAEL
		ORF1ab_1675	YLATALLTL
		ORF1ab_3013	SLPGVFCGV
		ORF1ab_3467	VLAWLYAAV
		ORF1ab_3482	FLNRFTTTL
		ORF1ab_3710	TLMNVLTLV
		ORF1ab_3732	SMWALIISV
		ORF1ab_3871	VLLSVLQQL
		ORF1ab_4032	MLFTMLRKL
		ORF1ab_4094	ALWEIQQVV
		ORF1ab_4515	TMADLVYAL
		ORF1ab_4725	IFVDGVPFV
	S	S_269	YLQPRTFLL
		S_691	SIIAYTMSL
		S_821	LLFNKVTLA
		S_976	VLNDILSRL
		S_983	RLDKVEAEV
		S_1000	RLQSLQTYV
		S_1220	FIAGLIAIV
HLA-B*40:01	N	N_322	MEVTPSGTWL
	ORF1ab	ORF1ab_1705	GEAANFCAL
		ORF1ab_2325	AEWFLAYIL
		ORF1ab_744	GETLPTEVL
		ORF1ab_1548	GEVITFDNL
		ORF1ab_2069	TEVVGDIIL
	S	S_153	MESEFRVYS
		S_168	FEYVSQPFL
		S_505	YQPYRVVVL
		S_582	LEILDITPC
		S_618	TEVPVAIHA
		S_1016	AEIRASANL
		S_1257	DEDDSEPVL
HLA-DRB1*15:01	M	M_91	MWLSYFIASFRLFAR
		M_166	KEITVATSRTLSYYK
	N	N_301	WPQIAQFAPSASAFF
		N_346	FKDQVILLNKHIDAY
	ORF1ab	ORF1ab_471	EEIAIILASFSASTS
		ORF1ab_5016	RAMPNMLRIMASLVL
	S	S_51	TQDLFLPFFSNVTWF
		S_56	LPFFSNVTWFHAIHV
		S_191	EFVFKNIDGYFKIYS
		S_236	TRFQTLLALHRSYLT
		S_896	IPFAMQMAYRFNGIG

Supplementary Table 1. List of SARS-CoV-2 epitopes evaluated in this study. Spheromers displaying these peptides in context of the indicated MHC-I/II proteins were used to study the $CD8^+$ and $CD4^+$ T cell responses against the SARS-CoV-2 proteins (Wuhan-1 strain). The table shows the HLA-restriction, source protein, epitope start number and peptide sequence. Related to STAR Methods.

Supplementary figure 1

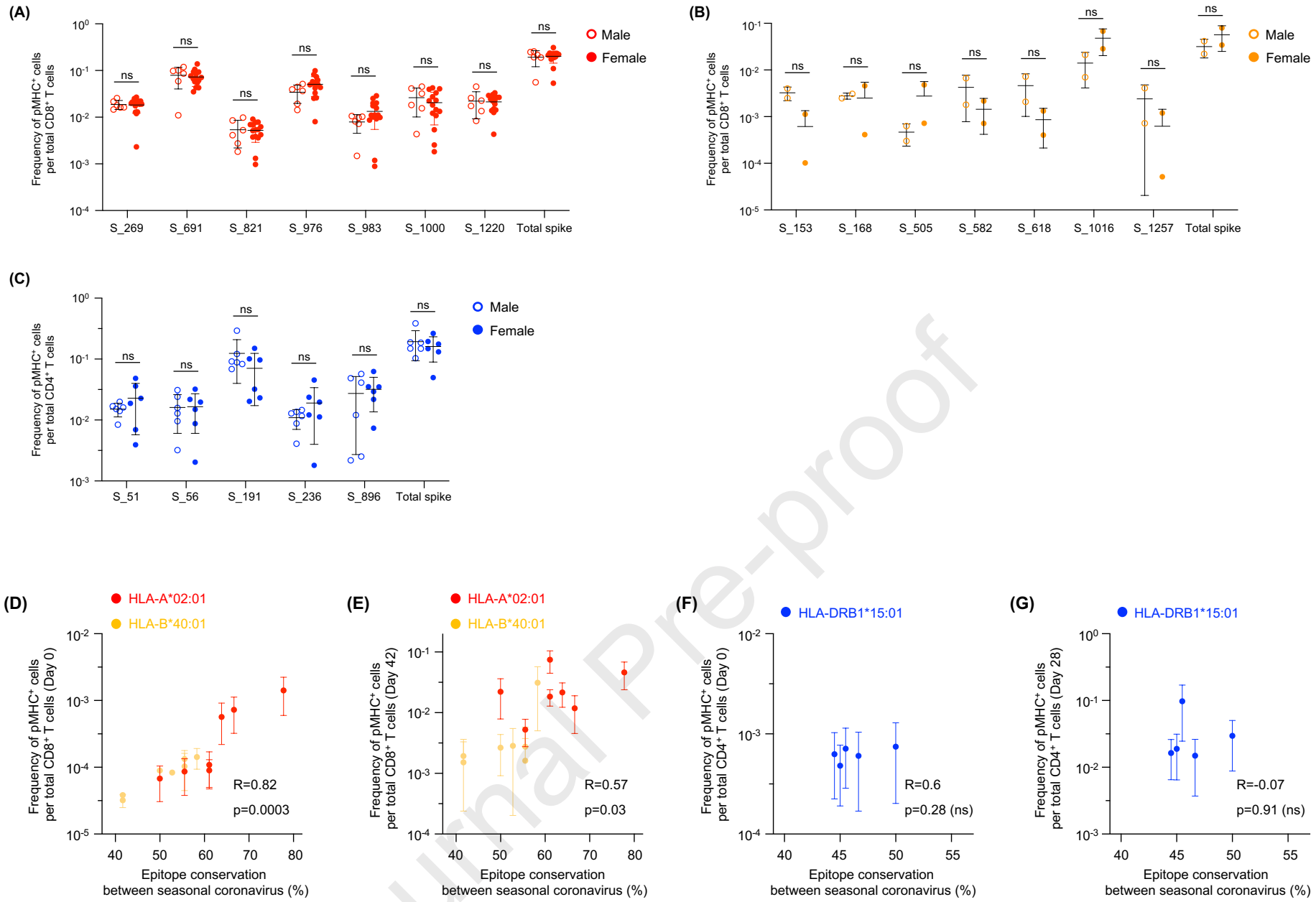

Supplementary figure 1. Correlation between spike-specific T cell response, sex and epitope conservation. (A and **B)** Correlation between epitope specific CD8⁺ T cell response (day 42) and sex in **(A)** HLA-A*02:01 and **(B)** HLA-B*40:01 restricted vaccinees. **(C)** Correlation between epitope specific CD4⁺ T cell response (day 28) and gender in HLA-DRB*15:01 restricted vaccinees. **(D)** Correlation between baseline spike-specific CD8⁺ T cell response (day 0) and the conservation of tested epitope. **(E)** Correlation between peak spike specific CD8⁺ T cell response (day 42) and the conservation of tested epitope. **(F)** Correlation between baseline spike specific CD4⁺ T cell response (day 0) and the conservation of tested epitope. **(G)** Correlation between peak spike specific CD4⁺ T cell response (day 28) and the conservation of tested epitope. Data are presented as mean ± SD. P values were determined by Mann–Whitney test with Holm–Šídák method. Related to Figure 1 and 2.

Supplementary figure 2

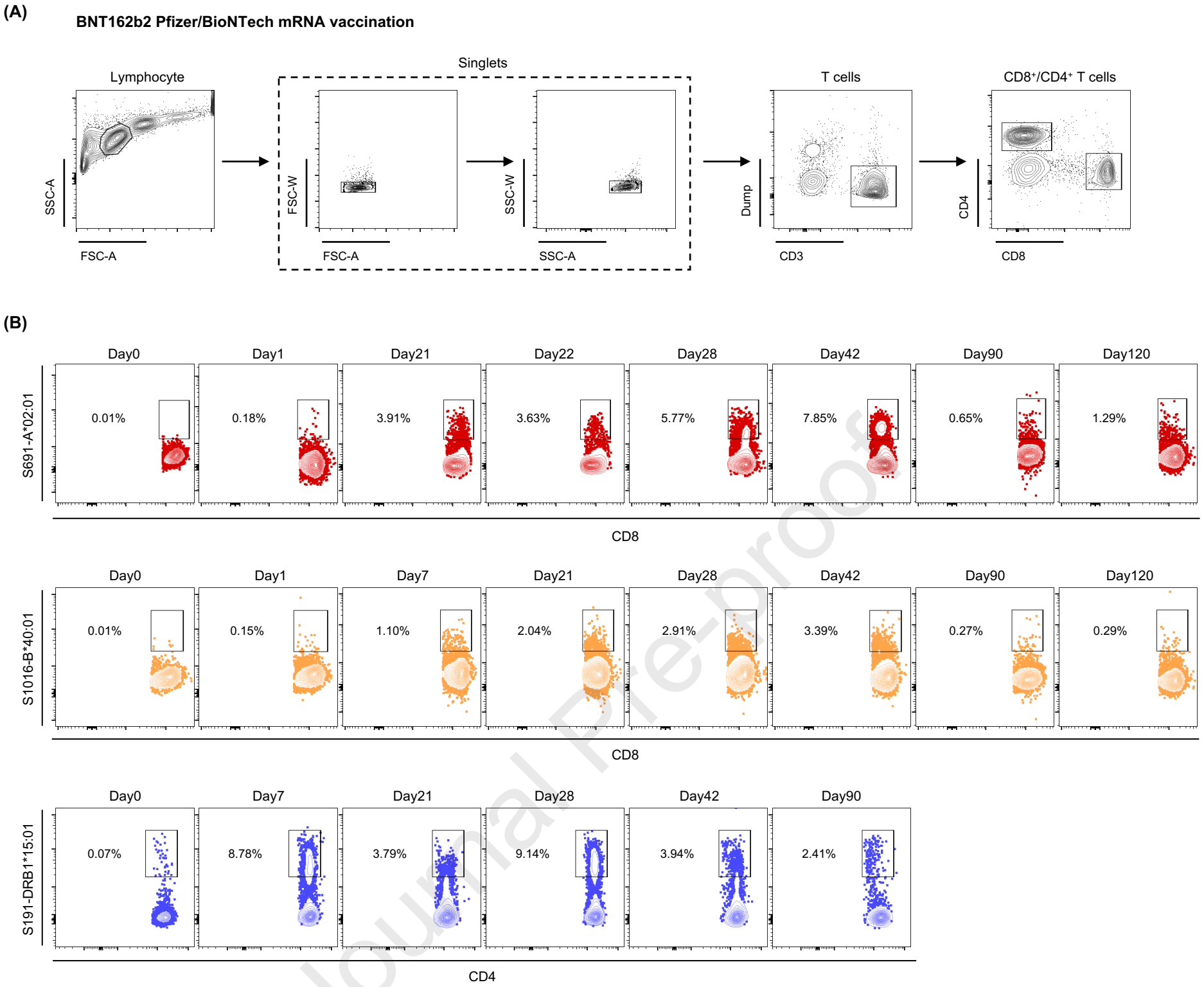

Supplementary figure 2. Representative FACS plots of epitope-specific CD8⁺ and CD4⁺ T cells after spheromer staining. **(A)** Gating strategy and **(B)** representative FACS plots of dominant epitopes HLA-A*02:01/S691 (upper panel) HLA-B*40:01/S1016 (middle panel) and HLA-DRB1*15:01/S191 (lower panel) from SARS-CoV-2 naïve vaccinees. Related to Figure 1 and 2.

Supplementary figure 3

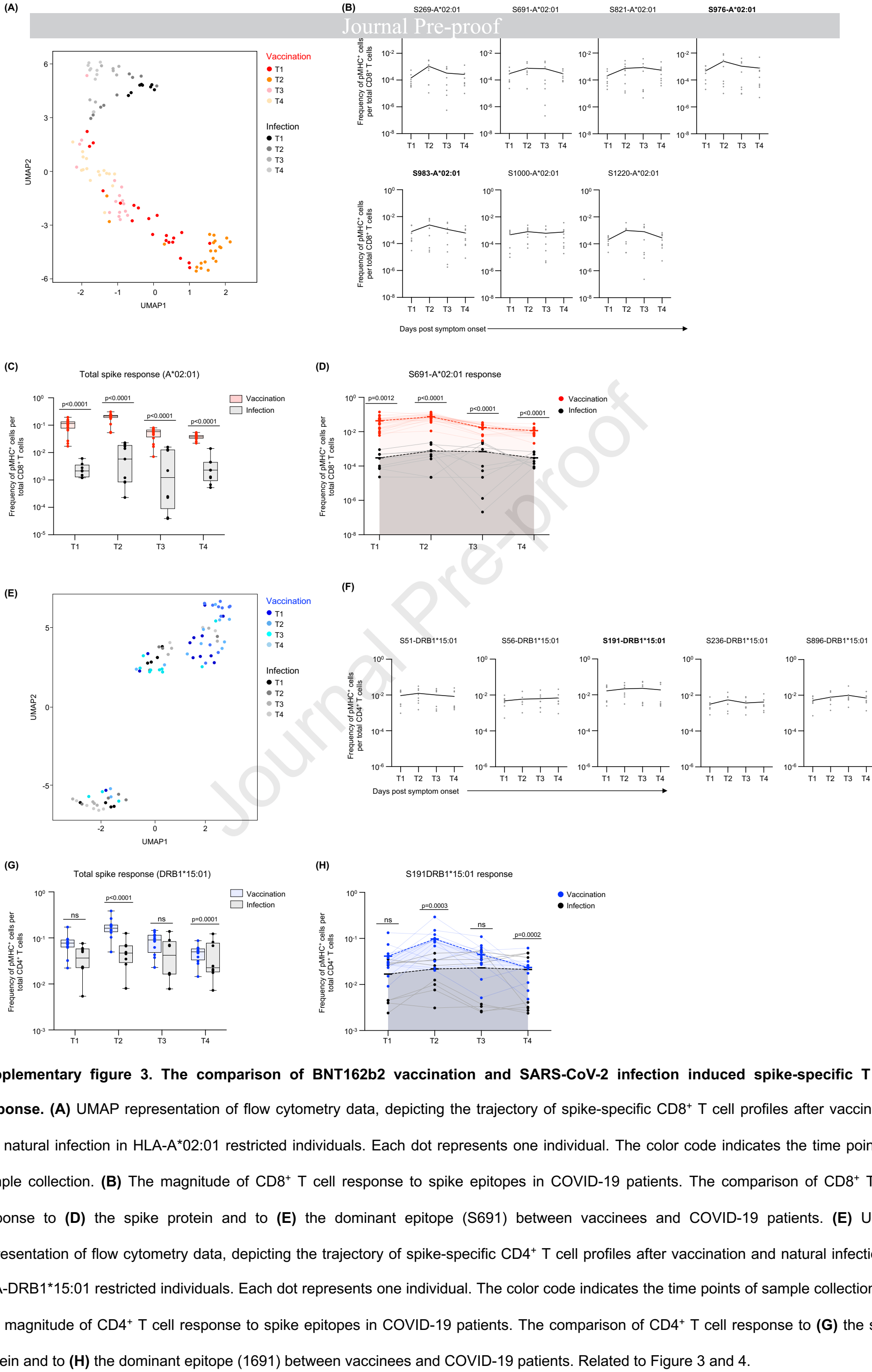

Supplementary figure 3. The comparison of BNT162b2 vaccination and SARS-CoV-2 infection induced spike-specific T cell response. (A) UMAP representation of flow cytometry data, depicting the trajectory of spike-specific CD8⁺ T cell profiles after vaccination and natural infection in HLA-A*02:01 restricted individuals. Each dot represents one individual. The color code indicates the time points of sample collection. **(B)** The magnitude of CD8⁺ T cell response to spike epitopes in COVID-19 patients. The comparison of CD8⁺ T cell response to **(D)** the spike protein and to **(E)** the dominant epitope (S691) between vaccinees and COVID-19 patients. **(E)** UMAP representation of flow cytometry data, depicting the trajectory of spike-specific CD4⁺ T cell profiles after vaccination and natural infection in HLA-DRB1*15:01 restricted individuals. Each dot represents one individual. The color code indicates the time points of sample collection. **(F)** The magnitude of CD4⁺ T cell response to spike epitopes in COVID-19 patients. The comparison of CD4⁺ T cell response to **(G)** the spike protein and to **(H)** the dominant epitope (1691) between vaccinees and COVID-19 patients. Related to Figure 3 and 4.

Supplementary figure 4

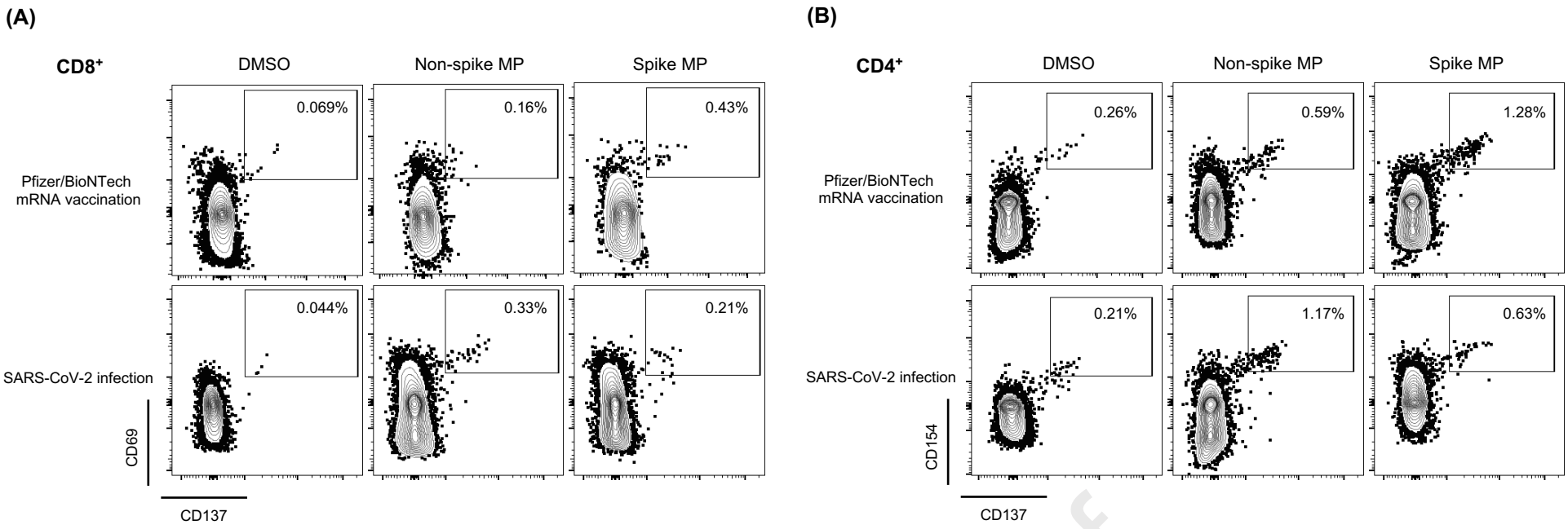

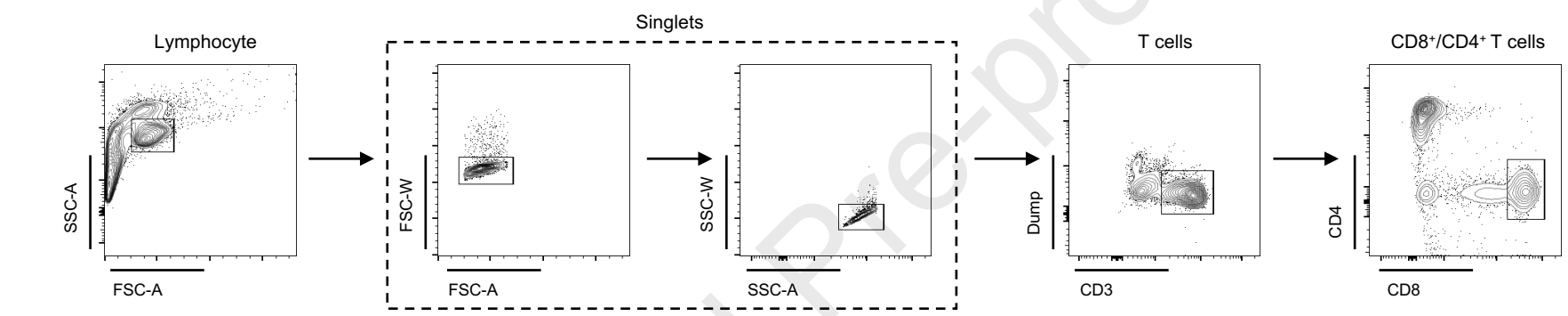

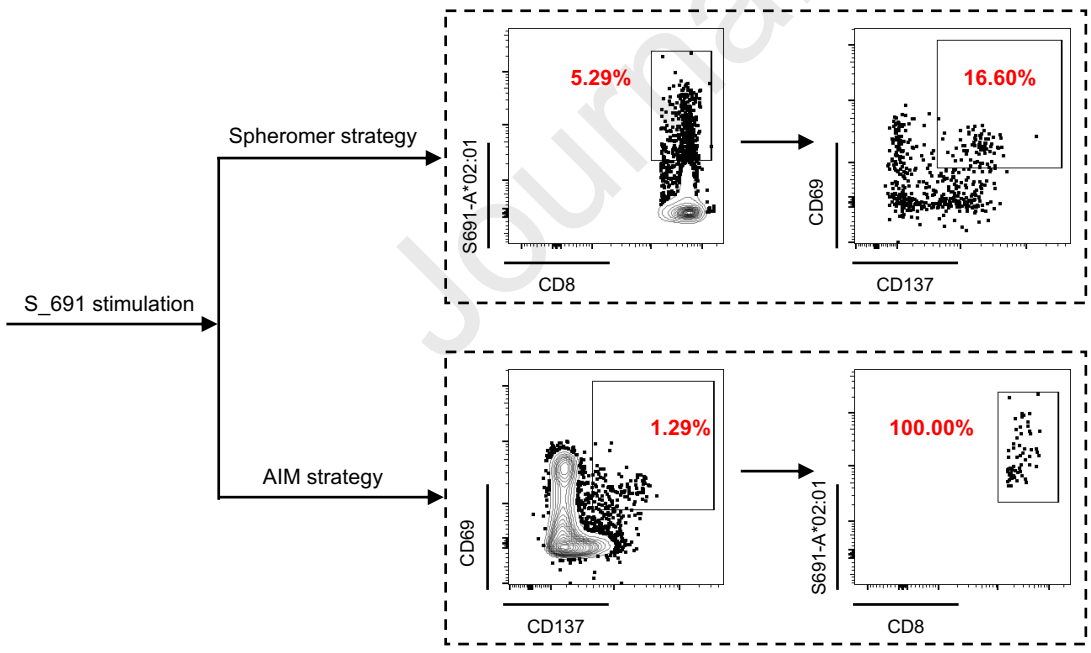

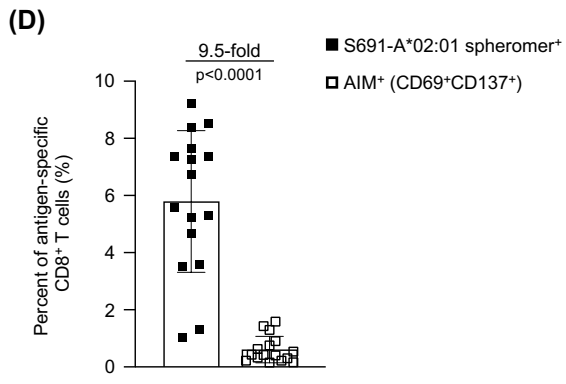

Supplementary figure 4. Antigen-specific CD8⁺ T cell measured by AIM assay. (A) and **(B)** Representative FACS plots of spike and non-spike specific CD8⁺ and CD4⁺ T cells after peptide mega pools (MPs) stimulation. PBMCs of SARS-CoV-2 naïve vaccinees (day 42) and COVID-19 patients (T2) were stimulated with the spike MP, non-spike MP or DMSO. The gating strategy for the AIM assay is illustrated by representative plots defining spike-specific and non-spike-specific **(A)** CD8⁺ and **(B)** CD4⁺ T cells by expression of CD69⁺CD137⁺ and CD154⁺CD137⁺, respectively. **(C)** and **(D)** The comparison of antigen-specific CD8⁺ T cell captured by spheromer staining and AIM assay. **(C)** Gating strategy of spheromer staining (upper panel) and AIM assay (lower panel) after peptide (S691) stimulation of day 42 PBMCs samples in HLA-A*02:01 restricted naïve vaccinees. **(D)** The frequency of HLA-A*02:01/S691 specific CD8⁺ T cells captured by spheromer staining and AIM assay. Data are presented as mean ± SD. Related to Figure 3 and 4.

Supplementary figure 5

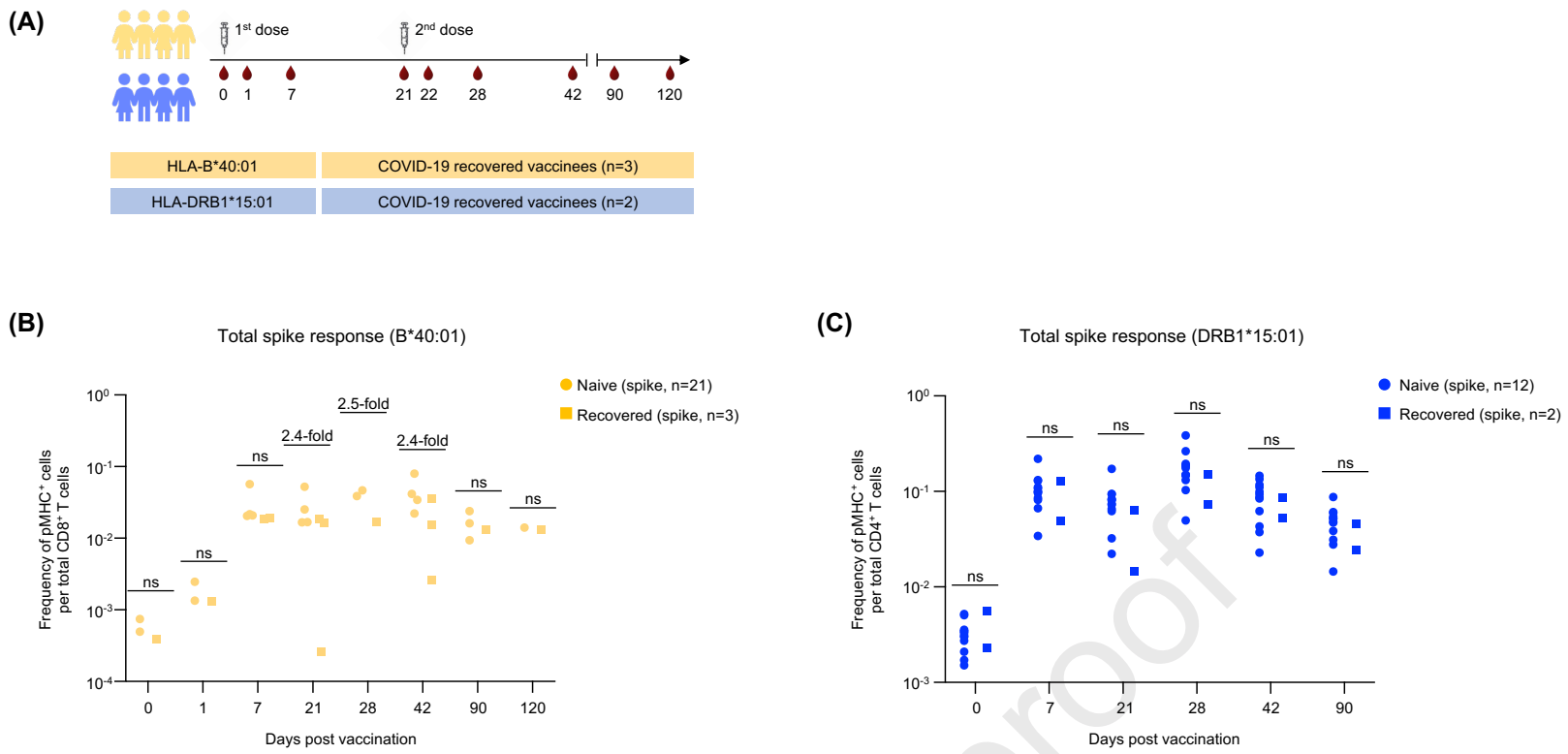

Supplementary figure 5. The magnitude of vaccine-elicited CD8⁺ and CD4⁺ T cell responses to spike epitopes in recovered COVID-19 patients. (A) Experimental design to study the longitudinal epitope-specific CD8⁺ and CD4⁺ T cell responses to BNT162b2 vaccine in vaccinees recovered from previous COVID-19 infection. Timeline indicating the collection of sequential blood samples from HLA-B*40:01 (day 0, 1, 7, 21, 28, 42, 90 and 120) and HLA-DRB1*15:01 (day 0, 7, 21, 28, 42 and 90) restricted recovered vaccinees. The number of donors (n) is indicated. The comparison of **(B)** CD8⁺ and **(C)** CD4⁺ T cell responses to spike protein in naïve and recovered vaccinees. Data are presented as mean ± range. Related to Figure 5.